Journal of Medicinal Chemistry

Article

Discovery of a Novel Inhibitor of Histone Lysine-Specific Demethylase 1A (KDM1A/LSD1) as Orally Active Antitumor Agent

Paola Vianello, Oronza A Botrugno, Anna Cappa, Roberto Dal Zuffo, Paola Dessanti, Antonello Mai, Biagina Marrocco, Andrea Mattevi, Giuseppe Meroni, Saverio Minucci, Giulia Stazi, Florian Thaler, Paolo Trifiro', Sergio Valente, Manuela Villa, Mario Varasi, and Ciro Mercurio

J. Med. Chem., **Just Accepted Manuscript** • DOI: 10.1021/acs.jmedchem.5b01209 • Publication Date (Web): 24 Dec 2015

ACS Publications

Journal of Medicinal Chemistry is published by the American Chemical Society. 1155 Sixteenth Street N.W., Washington, DC 20036

Discovery of a Novel Inhibitor of Histone Lysine-Specific Demethylase 1A (KDM1A/LSD1) as Orally Active Antitumor Agent

Paola Vianello,[a] Oronza A. Botrugno,[a] Anna Cappa,[a] Roberto Dal Zuffo,[a] Paola Dessanti,[a] Antonello Mai,[c,d] Biagina Marrocco,[c] Andrea Mattevi,[b] Giuseppe Meroni,[a] Saverio Minucci,[a,e] Giulia Stazi,[c] Florian Thaler,[a] Paolo Trifiró,[a] Sergio Valente,[c] Manuela Villa,[a] Mario Varasi[a] and Ciro Mercurio[a,f]**

a. Department of Experimental Oncology, Academic Drug Discovery, European Institute of Oncology, Via Adamello 16, Milan 20139, Italy.

b. Department of Biology and Biotechnology, University of Pavia, Via Ferrata 1, 27100 Pavia (Italy).

c. Department of Drug Chemistry and Technologies, Sapienza University of Rome, P.le A. Moro 5, 00185 Roma (Italy).

d. Pasteur Institute - Cenci Bolognetti Foundation, Sapienza University of Rome, P.le A. Moro 5, 00185 Roma (Italy).

e. Department of Biosciences, University of Milan, Via Celoria, 26, 20133 Milan, Italy

f. Genextra Group, DAC s.r.l., Via Adamello 16, 20139 Milano, Italy

* Email correspondence to paola.vianello@ieo.eu, ciro.mercurio@ieo.eu

KEYWORDS: LSD1, KDM1A, epigenetics; leukemia; lysine-specific demethylase-1; tranylcypromine.

ABSTRACT

We report the stereoselective synthesis and biological activity of a novel series of tranylcypromine (TCPA) derivatives (**14a-k, 15, 16**), potent inhibitors of KDM1A. The new compounds strongly inhibit the clonogenic potential of acute leukemia cell lines. In particular three molecules (**14d**, **14e** and **14g**) showing selectivity *versus* MAO A and remarkably inhibiting colony formation in THP-1 human leukemia cells, were assessed in mouse for their preliminary pharmacokinetic. **14d** and **14e** were further tested *in vivo* in a murine acute promyelocytic leukemia model, resulting **14d** the most effective**.** Its two enantiomers were synthesized: the (1S, 2R) enantiomer **15** showed higher activity than its (1R, 2S) analogue **16**, both in biochemical and cellular assays. Compound **15** exhibited *in vivo* efficacy after oral administration, determining a 62% increased survival in mouse leukemia models with evidence of KDM1A inhibition. The biological profile of compound **15** supports its further investigation as a cancer therapeutic.

INTRODUCTION

Over the last two decades, the relevance of epigenetic modifications for transcriptional control and normal development, as well as the role of such modifications in cancer development and progression, has attracted a great deal of attention.[1-3] Histone lysine methylation, a dynamic and accurately regulated mechanism,[4, 5] represents one of the several post-translation modifications controlling chromatin conformation and gene transcription.[6] Two enzyme families, lysine methyltransferases (KMTs)[7] and demethylases (KDMs)[8, 9], control histone lysine methylation. KDMs encompass the Jumonji C (JmjC) domain–containing proteins[8] and the lysine specific demethylase (LSD) family[9].

Two lysine specific demethylase proteins have been identified to date: KDM1A (LSD1), a flavin adenine dinucleotide (FAD) dependent amino oxidase which was the first discovered histone

lysine demethylase[10], and its homologous KDM1B (LSD2)[11]. KDM1A is often found associated with protein complexes functioning as transcriptional repressors, such as CoRest[12-14], and with the nucleosome remodelling and deacetylation complex Nurd[15, 16]. Consistently, KDM1A demethylates mono and dimethyl histone 3 lysine 4 (H3K4me1, H3K4me2), which are marks associated with active gene transcription[17].

In addition, KDM1A has been found in complexes involved in active gene transcription and reported to change its substrate specificity from H3K4me1/me2 to mono and dimethyl histone H3 lysine 9 (H3K9me1/me2), once associated to estrogen and androgen nuclear receptors[18, 19]. KDM1A has also been found in protein complexes involved in transcription elongation such as the ELL complex[20] and the MLL super complex[21].

The H3K4 demethylase activity of KDM1A can be influenced by histone posttranslational modifications such as acetylation[22] and phosphorylation[23]. In particular, both histone H3 lysine 9 acetylation (H3K9Ac) and histone H3 serine 10 phosphorylation (H3S10p)[23] can strongly reduce or block KDM1A demethylase activity.

Several non histone substrates of KDM1A have been identified[24-28]. For instance, KDM1A demethylates and stabilizes DNA methyl transferase 1 (DNMT1)[27], E2F1[23] and STAT3[28]. Furthermore, KDM1A demethylates the myosin phosphatase MYPT1, a phosphatase involved in Rb dephosphorylation[24], as well as repressing p53 function through the inhibition of its interaction with 53BP[25].

High KDM1A expression correlates with poor prognosis in several tumor types such as neuroblastoma,[29] prostate cancer,[18, 30] non small cell lung cancer,[31] breast cancer,[32, 33] esophageal squamous cancer[34], and hepatocellular carcinoma[35]. Bladder cancer[36] and colorectal cancer[37] are also characterized by elevated KDM1A expression. Notably, KDM1A was recently proposed to

confer stem cell like characteristics upon breast cancer cells[38] as well as maintain stem cell-like tumor propagating cells in human glioblastoma[39]. In hematopoietic and lymphoid neoplasias, high expression of KDM1A has been observed in acute myeloid leukemia[40], myeloproliferative neoplasms, chronic myelomonocytic leukemia, and myelodysplastic syndromes[41]. In addition, strong experimental evidence supports a role for KDM1A in the self-renewal of leukemic stem cells in acute myeloid leukemia (AML), and, more specifically, in the promotion of the oncogenic gene program associated with MLL-AF9 leukemia[42].

The link between KDM1A and tumor pathogenesis, and the discovery that the monoamine oxidase (MAO) inhibitor tranylcypromine (TCPA) blocks KDM1A activity[22], represented the starting point for intensive drug discovery programs aimed at the development of irreversible TCPA-based KDM1A inhibitors[43-56]. Two TCPA derivatives (Figure 1), N4-[(1R,2S)-2-phenylcyclopropyl]cyclohexane-1,4-diamine (**22**, ORY1001/RG-6016)[57-59] and 4-[[4-[[[(1R,2S)-2-phenylcyclopropyl]amino]methyl]-1-piperidyl]methyl]benzoic acid (**23**, GSK2879552)[60-62], both characterized by nitrogen substitution at the core of TCPA, are currently under clinical investigation. In addition, several reversible inhibitors of KDM1A have been identified by different research groups[63].

In a previous manuscript, we showed that substitutions on the phenyl moiety of TCPA allowed the identification of highly active KDM1A inhibitors[64]. Among these, compound **1** (4-benzamido-cyclopropylamine; **13b** in reference[64]) (Figure 2) demonstrated to be a potent KDM1A inhibitor, while its ortho and meta regioisomers exhibited a lower activity against KDM1A[65]. The enantiomers of compound **1** displayed potent KDM1A inhibition, with IC_{50} values ranging from 13 to 26 nM, as well as anticlonogenic activity in primary murine acute promyelocytic leukemia blasts. These results prompted us to expand the scaffold with the aim to

obtain compounds with a better selectivity profile towards MAO A and good activity in a human cellular model of MLL-AF9 leukemia (THP-1 cells). Compound **14d** was found to be the most promising derivative in this respect, and its biological properties encouraged the synthesis of its two enantiomers. We report herein the stereoselective synthesis of the two enantiomers (Scheme 1) together with their *in vitro* and *in vivo* characterization.

RESULTS AND DISCUSSION

Chemistry. The synthesis of the final compounds **14a-k**, **15** and **16** was carried out following two routes. According to Scheme 1 (Method A), the oxirane **2** as well its 2-S (**3**) and 2-R (**4**) analogues were added to a solution of triethyl phosphonoacetate and butyl lithium in dimethoxyethane and the reaction was microwave irradiated to 130°C affording the ethyl esters of 2-phenylcyclopropanecarboxylic acids. Subsequent hydrolysis of the ethyl esters with LiOH provided the carboxylic acids **5-7**, which were treated with iodine in acetic acid yielding the 4-iodo derivatives **8-10**. The protected amino derivatives **11-13** were subsequently obtained by reaction of the iodo derivatives **8-10** with diphenyl phosphorazidate (DPPA) in presence of triethylamine and in tert-butanol at 90°C. Ullman reaction with primary amides and subsequent BOC deprotection with hydrochloric acid afforded the cyclopropylamines **14a-g, 15** and **16** as their hydrochloride salts.

According to Scheme 2 (Method B), the appropriate acids **18h-k** were activated by benzotriazol-1-yl-oxytripyrrolidinophosphonium hexafluorophosphate (PyBOP) or 1-(3-dimethylaminopropyl)-3-ethylcarbodiimide (EDC), in the presence triethylamine and condensated with *tert*-butyl *N*-[2-(4-aminophenyl)cyclopropyl]carbamate **17**[64]. The final compounds **14h-k** were smoothly obtained by removing Boc protection with hydrochloric acid in dioxane.

The carboxylic acid or primary amide intermediates were prepared according to Schemes 3 or 4 when not commercially available.

The synthesis of bisubstituted acids **18h-k** is reported in Scheme 3. *tert*-Butyl chloro-nitro-benzoates[66] were converted into **19h-k** by reaction with morpholine, 4-methylpiperazine, or piperidine in presence of K_2CO_3. Reduction of the nitro group to the amine in compounds **20h-k** was achieved by conventional catalytic hydrogenation, e.g. in a Parr hydrogenation or H-Cube apparatus using a palladium catalyst. The carbamates **21h-k** were then obtained by reacting the free amines **20h-k** with benzyl chloroformate in presence triethylamine at room temperature. Finally, the *tert*-butyl ester group was hydrolyzed with TFA (trifluoroacetic acid) in dichloromethane.

The benzamides **19e-f** were prepared according to Scheme 4. The commercially available 3- or 4-(2-oxo-1,3-oxazolidin-3-yl)benzoic acids **18e** and **18f** were first activated with thionyl chloride and then converted into the amides **19e-f** with aqueous NH_3 in DMF.

Biological Evaluation and SAR,. Benzamido-derivatives of TCPA have been previously described, reporting the para substitution more potent than the ortho and meta isomers.[56, 64, 65] Substituents on the phenyl ring of compound **1** were directed towards a major occupancy of the binding pocket, without impacting on drug like properties of the molecules, thus maintaining solubility at an acceptable level. For this purpose, both aliphatic (piperazine, morpholine, piperidine oxazolidin-2-one) and aromatic (furane) heterocycles were prioritized among the set of most frequently used ring systems present in small molecule drugs[67]. Alternatively or concurrently we introduced a carbobenzyloxy residue which could either impact on the stereoelectronic features of the benzamide end side, or branch the molecule to modulate selectivity *versus* MAOs.[56] As summarized in Table 1 the final compounds **14a-k** as well as the

reference compound **22** were profiled *in vitro* for their KDM1A, KDM1B, MAO A and B inhibitory activities. To this end human recombinant KDM1A/CoREST and KDM1B as well as MAO A and MAO B proteins were employed as enzymatic sources. The compounds were incubated with the enzymatic complex and the results are expressed as IC_{50} values.

The introduction of different residues did not lead to further increase in KDM1A inhibitory activity, the most potent being the equipotent furan-bearing **14a** (IC_{50} =0.022 μM to be compared to 0.019 μM of compound **1**). However all compounds showed IC_{50} values equal to or less than 0.1 μM, with the exception of compound **14k** (IC_{50}=0.308 μM). Similarly, substitution in meta *versus* para did not influence the inhibitory potency of KDM1A (**14e** vs **14f**), whereas the use of carbobenzyloxy group **14b** gave a 2 fold less potent derivative, which slightly improved in its cyclized analogue meta oxazolidin-2-one **14e**. The para oxazolidin-2-one derivative **14f** resulted two times more potent than the morpholine analogue **14c,** which in turn was 3 fold more potent than piperazine **14d**. Furthermore, substitution of the benzamide, in particular by a 3-benzyloxycarbonylamino (3-CBZ) moiety resulted in an increased KDM1B inhibitory activity. In specific, compound **1** exhibited an IC_{50} value of 58.3 μM, the 3-CBZ substituted derivative **14b** resulted to be roughly five times more active (IC_{50}=11.6 μM), while the disubstituted inhibitors **14h**, **14j**, and **14k** had IC_{50} values of around 5 μM. With the exception of **14a**, having an IC_{50} value of 0.09 μM, all other compounds were selective over MAO B: in particular, compounds **14b**, **14g** and **14j** did not show any MAO B inhibitory activity under the employed experimental conditions. We hypothesized that the higher activity of **14a** *versus* MAO B can be related to the aromaticity of the furan, which finds an ideal environment in the highly hydrophobic active site of MAO B.[68] MAO A IC_{50}s ranged between 0.025 μM (**14b**) and 1.0 μM (**14j**), among them **14d**,**14e** and **14g-j** resulted to be more selective than compound **1** (MAO

A/KDM1A ratio < 2). **14g** and **14j** resulted to be the most selective ones, with a selectivity ratio higher than 10 (MAO A/ KDM1A).

The compounds with good biochemical activity and with an acceptable selectivity *versus* MAO A were selected and further tested them towards leukemia cell lines to investigate their ability to inhibit KDM1A: **14d**, **14e** and **14g-j** (see Table 2). In a first experiment, human promyelocytic leukemia NB4 cells were incubated with the inhibitors at a concentration equal to their corresponding biochemical IC_{50} value. NB4 cells were selected on the basis of literature data[64, 69] which indicate that the inhibition of KDM1A has a biological relevance both in human promyelocytic leukemia cell lines (NB4) and murine primary promyelocytic blasts. After 24 hours of incubation, GFI1B mRNA levels were measured by quantitative RT-PCR to measure KDM1A inhibition in cells. GFI1B is a gene associated to hematopoietic differentiation, its mRNA expression increases following KDM1A down regulation (Figure S2 supplementary data) and more importantly the gene has been demonstrated to be a direct transcriptional target of KDM1A[70]. As shown in Table 2, all the tested compounds determined at least a 4-fold increase of the mRNA expression of GFI1B, compared to cells treated with the vehicle, proving their ability to block KDM1A activity in cellular systems. Moreover, considering that KDM1A inhibition should induce differentiation of human AML cells [40] we evaluated the effect of the compounds on the expression level of CD11b, a well known granulocytic differentiation marker modulated by KDM1A dowregulation (Fig.S2 supplementary data). As reported in Table 2, all the tested compounds elicited, at their respective biochemical $IC_{50,}$ an increase of CD11b expression, suggestive of granulocytic differentiation induction of the NB4 cells. Starting from experimental data[64, 69], which indicate that the KDM1A inhibitors are of potential relevance for treatment of promyelocytic leukemia, we further investigated the cellular activity of the

compounds by measuring their ability to inhibit the colony formation of murine acute myeloid leukemia blasts (originated by a murine acute promyelocytic leukemia[71]) in semisolid culture at a dose of 0.250 μM. All the selected compounds inhibited colony formation, the percentage of inhibition ranging from 84 to 57% (Table 2). To confirm that the obtained biological data specifically correlated to KDM1A inhibition, the effect of KDM1A down regulation by shRNA, both in NB4 cells and murine promyelocytic blast, was analyzed. As reported in the supplementary section, the effect of KDM1A silencing are in agreement with the reported biological data obtained with the inhibitors both in terms of transcriptional effects on the expression of GFI1B and CD11b and on the reduction of colony formation in mouse acute promyelocytic blast (supplementary data Figure S2 and S3).

The most active compounds **14d, 14e** and **14g,** inhibiting the murine promyelocytic blasts at 84 and 79% respectively, as well as the reference compound **1** (inhibition of 73%) and **22** (inhibition of 84%), were additionally tested in a human leukemia cell line. Since the relevance of KDM1A in sustaining the oncogenic potential of MLL-AF9 leukemia stem cells has been demonstrated and reported in the literature[40], we evaluated the anticlonogenic potential of **14d**, **14e**, **14g, 1** and **22** in a human leukemia cell line, characterized by MLL-AF9 translocation (THP-1). As reported in Table 2, compounds **14d**, **14e** and **14g** as well as **22** continued to show strong inhibitory efficacy with a percentage of inhibition of 63, 51, 65 and 58 % respectively, at the fixed dose of 0.50 μM, whereas reference compound **1** unexpectedly only weakly inhibited the colony forming ability formation of the cells (8%). Of relevance, **14d**, **14e** and **14g** similarly to **22**, induced a clear differentiation of THP-1 cells as demonstrated by altered morphology of the colonies and by examination of cytospin preparations of cells recovered at the end of semi-solid culture (Figure 4).

We therefore advanced through our screening funnel only those compounds with good potency in the biochemical assay, showing some level of selectivity versus MAO A and demonstrating a clear cellular efficacy in the anticlonogenic potential assay. In view of their promising overall activity in both biochemical and cellular assays **14d**, **14e** and **14g** were selected for preliminary pharmacokinetic assessment in mouse, (Table 3) whilst the parent compound **1** was not included in the analysis for its very limited anticlonogenic activity observed in THP-1 cells.

The selected inhibitors were administered in single intravenously (iv) or orally (os) to CD1 mice at 5 mg/kg or 15 mg/kg respectively. The derivatives were dissolved in 5% glucose solution containing 10% tween 80 for the iv dose or in 5% glucose solution containing 40% PEG for the oral dose. The plasma PK parameters are summarized in Table 3. Following the iv administration, the three compounds showed medium to high clearance rates of 94.8±21.3, 49.7±12.2 and 80.7±4.8 mL/min/kg for **14d**, **14e** and **14g** respectively. The elimination half-lives were significantly longer for **14d** (with ~8 h) and for **14g** (~12 h) than for compound **14e** (1.92±0.40 h). Moreover, the estimated terminal volume of distribution (V_z) was high for all three compounds, which indicates an extensive tissue distribution of the molecules. In particular, **14d** and **14g** had V_z of 67 and 85 L/kg, respectively, much higher than **14e** (V_z=8.45±3.75 l/kg). Compounds **14d** and **14g** were slowly absorbed after oral administration (t_{max} were 12 h and 18 h for **14d** and **14g**, respectively), whereas - **14e** was taken up more rapidly (t_{max} of less than 1 h). C_{max} and $AUC_{0-\infty}$ after oral administration were significantly different among the compounds. In specific, compound **14e** exhibits a C_{max} of 1.14±0.16 μM, which is around 20 times more than that obtained for compound **14g**. The $AUC_{0-\infty}$ ranged from 0.979±0.131 μMh (**14g**) to 7.12±2.04 μMh (**14e**). The higher exposure data after oral administration of **14d** and **14e** compared to **14g**, both in terms of C_{max} and $AUC_{0-\infty,}$ and the higher oral bioavailability of compounds **14d** (40%)

and **14e** (55.8%) compared to **14g** (15.4%) prompted us to select **14d** and **14e** for a further *in vivo* characterization.

To this aim, **14d** and **14e** were submitted to *in vivo* efficacy experiment in an established murine promyelocytic leukemia model.[71, 72] For the *in vivo* test, one million leukemic cells were injected iv into non-irradiated 129SvEv mice. Treatment with **14d** and **14e** started once blast cells were detected in the recipients' peripheral blood (10 days after cell injection). To compare the efficacy between the two selected compounds, **14d** and **14e** were orally administered at the fixed dose of 27 mg/kg five days per week for two weeks. The survival of mice belonging to different experimental groups was analyzed and represented by a Kaplan–Meier survival plot. No significant body weight differences among the groups of mice were observed during the treatment (data not shown) and, as reported in figure 5, both compounds elicited an increase of survival of the treated mice compared to the vehicle group. Specifically, **14d** and **14e** determined an increase of survival respectively of 35 and 15% with respect to the vehicle group. At this point, to investigate different schedule of compound administration for the *in vivo* efficacy, we considered the irreversible mechanism towards which these derivatives interact with the enzyme and we postulated that an intermittent treatment could have been desirable. **14d** in fact was tested at the dose of 45 mg/kg for three days per week (Monday, Tuesday and Wednesday) for two weeks that correspond to the same weekly cumulative dose obtained with the administration of the compound at the dose of 27 mg/kg for 5 days per week. Interestingly, the *in vivo* efficacy evaluated in terms of survival improved significantly (from 35 to 58%) when we followed the intermittent administration (Figure 5B). Moreover and importantly, **14d** shown a significant better *in vivo* efficacy in the murine promyelocytic leukemia model if compared to **22** which,

once administered according to schedule/dosage reported by Oryzon[73] was able to increase the survival of leukemic mice of 14% with respect to the vehicle group (Figure 5C).

Furthermore, in order to correlate the observed *in vivo* efficacy with KDM1A inhibition, spleens of the leukemic mice treated with the vehicle and those with **14d** were recovered after 3 days of treatment and cells were collected for RNA analysis. mRNA levels of GFI1B were measured by quantitative RT-PCR using specific primers and normalized against TBP mRNA. Results are presented as mRNA expression and as illustrated in the graph (Figure 5D) both schedules determined a clear increase of GFI1B expression, although not statistically significant, supporting the ability of compound to inhibit KDM1A *in vivo* after oral administration.

Encouraged by the results on the racemic mixture of compound **14d**, we approached the enantioselective synthesis of **15** (1S, 2R) and **16** (1R, 2S) starting from the enantiomerically pure styrene epoxides. As evidenced in Table 4, compound **15** resulted to inhibit KDM1A with an IC_{50} of 0.084uM thus three times more potent than the enantiomer **16** (IC_{50}=0.23uM), which in turn was a weaker inhibitor with respect to the racemate (IC_{50}=0.188uM). The activity of the racemate and enantiomers versus KDM1B could be considered comparable, being in the high micromolar range. Selectivity versus MAOs remained instead almost unaltered in term of IC_{50}-ratio for the (1S, 2R) enantiomer (ratio MAO A/LSD1=3.5 for **15**, to be compared to 3.9 for **14d**) whereas it worsens for compound **16**. An even greater difference among the enantiomers was found in the cellular assays: specifically compound **15** resulted to be more active in reducing the colony forming ability in the two used cell models, and, importantly, in inducing the differentiation of THP-1 cells compared to the 1R, 2S analogue **16** (Table 5 and Figure 6).

Compound **15** was then evaluated for its *in vivo* behavior. For this purpose, the pharmacokinetic profile in CD-1 mice was analyzed at the same conditions formerly described for inhibitors **14d**,

14e and **14g** (Table 6). The compound exhibited a high clearance rate, but somewhat lower than the racemic mixture **14d** (79.7±15.0 mL/min/kg for **15** over 94.8±21.3 mL/min/kg for **14d**). Furthermore **15,** when orally administered, exhibited a high V_z of 58.4±9.78 L/kg and a half life of more than 8 h. Although the oral bioavailability was lower than that shown by **14d** (22.5% for **15** over 40% for **14d**) both C_{max} and $AUC_{0-\infty}$ were comparable (0.147±0.112 and 1.66±0.889 of **15** over 0.138±0.0517 and 2.39±0.770 of **14d**).

The single 1S,2R enantiomer **15** was tested *in vivo* in the murine promyelocytic leukemia model as previously described for the trans racemate **14d**. **15** was dissolved (40% PEG 400 in a 5% glucose solution) and orally administered 3 days per week (Monday, Tuesday and Wednesday) for 3 weeks at the doses of 11.25 mg/kg and 22.5 mg/kg. The treatment started once blast cells were detected in the recipients' peripheral blood (10 days after cell injection). As reported for the racemic mixture **14d**, the survival of mice of the different experimental groups was analyzed and represented by a Kaplan–Meier survival plot. No significant body weight differences among the groups of mice were observed during the treatment. A significant dose dependent increase of survival was obtained and, specifically, **15** determined an increase of 35 and 62% at the dose of 11.25 and 22.50 mg/kg respectively (Figure 7A). Remarkably the observed *in vivo* efficacy associated to a good tolerability profile of the compound **15** could be suggestive of its preferential activity on tumor cells with respect to normal cells. In order to correlate the observed *in vivo* efficacy of **15** with KDM1A inhibition, spleens of the leukemic mice treated with the vehicle or with compound at the highest tested dose of 22.5 mg/kg were recovered after 3 days of treatment and cells were collected for RNA analysis. A clear increase of GFIB expression, although not statistically significant, was observed (Figure 7B), which supported the ability of **15** to inhibit KDM1A *in vivo* after oral administration.

CONCLUSIONS

A series of novel and potent TCPA-derived inhibitors of KDM1A has been identified starting from the previously disclosed compound **1**. Some of the compounds (**14d**, **14e** and **14g**) demonstrated improved selectivity *versus* MAO A and a higher cellular activity in human THP-1 cells, showing 51-65% inhibition compared to the 8% inhibitory activity of compound **1**. Pharmacokinetic studies revealed a good oral bioavailability of compounds **14d** (40%) and **14e** (55.8%), in both cases significantly higher than that of derivative **14g** (15.4%). Compounds **14d** and **14e** were then studied for their *in vivo* antitumoral activity in a murine acute promyelocytic leukemia model. Oral treatment with compounds **14d** and **14e**, at the fixed dose of 27 mg/kg five days per week for two weeks, led to significant survival increase without signs of overt toxicity and with evidence of *in vivo* target modulation. Two enantiomers of **14d** were eventually prepared and profiled, leading to the identification of the (1S, 2R) eutomer **15**, which showed higher potency in both biochemical and cellular assays in comparison to the (1R, 2S) enantiomer **16**.

Compound **15,** orally admistered *in vivo* in the murine promyelocytic leukemia model, was well tolerated and significanly prolonged survival time of the treated mice (35 and 62% at the doses of 11.25 and 22.50 mg/kg, respectively). Collectively, these results have supported the progress of compound **15** into preclinical development as a potential oral anticancer agent.

EXPERIMENTAL SECTION

Chemistry

General Procedures.Reagents and solvents used, unless stated otherwise, were of commercially available reagent grade quality and were used without further purification. Flash chromatography purifications were performed on Merck silica gel 60 (0.04e0.063 mm). Nuclear magnetic

resonance spectra (^{1}H NMR and ^{13}C NMR) were recorded either on a Varian 500 MHz or on a Varian 400 MHz spectrometer at 300 K and are referenced in ppm (δ) relative to TMS. Coupling constants (J) are expressed in hertz (Hz). HPLC-MS experiments were performed on an Acquity UPLC apparatus, equipped with a diode array and a Micromass SQD single quadruple (Waters). Optical rotations were measured at the sodium D line, using a Krüss P3001/3002 RS automatic digital polarimeter and a 100 mm cell and are reported as follows: concentration (c = g/100 mL), solvent. Purity was monitored at 220 nm and the purities of the compounds used for biological tests were found to be at least 95%.

Materials. *tert*-butyl *N*-[2-(4-aminophenyl)cyclopropyl]carbamate (48), *tert* butyl 3-chloro-4-nitro-benzoate[66], 4-(3-furyl)benzamide[74] benzyl N-(3-carbamoylphenyl)carbamate[75] were prepared according to procedures described in the literature. **22** was prepared according to the procedure decribed by Oryzon.[55]

(1R,2R)-1-Ethyl-2-phenylcyclopropanecarboxylate (6)

69 mL (173 mmol) of a 2.5 M solution of n-butyllithium in hexane was added at 25 °C dropwise over 5 min to a solution of 39 g (170 mmol) triethyl 2-phosphonoacetate in 75 mL of dry DME. The reaction mixture was stirred at RT for 5 min, then 16.0 g (133 mmol) of (*S*)-styrene oxide was added in one portion. The reaction was heated at 135°C for 60 min under MW. The orange reaction mixture was then cooled down to RT, saturated aqueous NH_4Cl was added and the product was extracted with Et_2O. The combined organic layers were dried over Na_2SO_4, filtered and the solvent was removed in vacuo. The crude product was filtered on a silica gel pad giving 21g (83%) of ethyl 2-phenylcyclopropane carboxylate as yellow oil.

The ethyl ester was hydrolized according to the following procedure: 10.58 g (441.6 mmol) LiOH in 200 mL of H_2O was added to a solution of 21 g (110 mmol) of ethyl 2-

phenylcyclopropanecarboxylate dissolved in 220 mL of an ethanol/THF mixture (10;1, v:v) and the solution was heated at 115°C for 50 min under MW irradiation. Then, the solution was concentrated, diluted with H_2O and quenched with 2 M HCl at 0°C. The precipitate was filtered off, washed with H_2O and triturated with Et_2O providing 14.85 g (83%) the (1R,2R) cyclopropane carboxylic acid **6** as a white solid. ^{1}H NMR ($CDCl_3$) δ (ppm): 11.5 (br s, 1 H, -COO*H*), 7.34–7.20 (m, 3 H, aromatic protons), 7.16–7.06 (m, 2 H, aromatic protons), 2.66–2.57 (m, 1 H, -C*H* cyclopropane), 1.98–1.88 (m, 1 H, -C*H* cyclopropane), 1.73–1.61 (m, 1 H, -C*H*H cyclopropane), 1.47–1.37 (m, 1 H, -CH*H*cyclopropane); MS (ESI): *m/z*: 161 $[M-H]^-$. $[\alpha]_D^{20}$ = -297° (c 0.753, $CHCl_3$).

The *trans*-1-ethyl-2-phenylcyclopropanecarboxylate **5** was purchased from Sigma-Aldrich **(1S,2S)-2-phenylcyclopropanecarboxylic acid 7** was prepared according to the procedure described for example **6** starting from the appropriate (*R*)-styrene oxides and phosphonoacetates Yield: 85%, ^{1}H NMR ($CDCl_3$) δ (ppm): 11.75 (br s, 1 H, -COO*H*), 7.35–7.08 (m, 5 H, aromatic protons), 2.67–2.56 (m, 1 H, -C*H* cyclopropane), 1.98–1.86 (m, 1 H, -C*H* cyclopropane), 1.74–1.63 (m, 1 H, -C*H*H cyclopropane), 1.48–1.37 (m, 1 H, -CH*H* cyclopropane); MS (ESI): *m/z*: 161 $[M-H]^-$. $[\alpha]_D^{20}$ = +294° (c 0.933, $CHCl_3$).

Examination of ethyl esters of **5**,**6** and **7** by NMR with the aid of the optically active shift reagent Europium tris[3-(heptafluoropropylhydroxymethylene)-(+)-camphorate], showed **5** to be a misture 1 to 1 of the two enantiomers, **6** and **7** to be optically pure **.**

(1R, 2R)-2-(4-iodophenyl)cyclopropanecarboxylic acid (9)

13 g (50 mmol) of iodine, 4.5 g (21 mmol) potassium iodate and 7.5 mL concentrated H_2SO_4 in 75 ml of H_2O was added to a stirred solution of 14.7 g (90.6 mmol) of (*1R,2R*)-2-phenylcyclopropanecarboxylic acid in 300 mL of AcOH. The mixture was heated to reflux for about 2 h, and then the reaction was stopped by adding 700 mL of 1 M $NaHSO_4$. The formed

precipitate was filtered, dried and the resulting solid was triturated with hexane providing 19 g (73%) of the (1R,2R) carboxylic acid **9** as a white solid. ^{1}H NMR (DMSO-d_6) δ (ppm): 12.66–10.65 (m, 1 H, -COO*H*), 7.72–7.54 (m, 2 H, aromatic protons), 6.96–6.79 (m, 2 H, aromatic protons), 2.63–2.46 (m, 1 H, -C*H* cyclopropane), 1.97–1.80 (m, 1 H, -C*H* cyclopropane), 1.74–1.61 (m, 1 H, -C*H*H cyclopropane), 1.47–1.30 (m, 1 H, -CH*H*cyclopropane); MS (ESI): *m/z*: 287 $[M-H]^-$.

The following carboxylic acids were prepared according to the procedure for compound **9**:

(*trans*)-2-(4-iodophenyl)cyclopropanecarboxylic acid (8)

Yield: 84% ^{1}H NMR (DMSO-d_6) δ (ppm): 12.36 (br s, 1 H, -COO*H*), 7.65–7.55 (m, 2 H, aromatic protons), 7.06–6.93 (m, 2 H, aromatic protons), 2.40–2.28 (m, 1 H, -C*H* cyclopropane), 1.85–1.73 (m, 1 H, -C*H* cyclopropane), 1.47–1.37 (m, 1 H, -C*H*H cyclopropane), 1.35–1.24 (m, 1 H, -CH*H* cyclopropane) MS (ESI): *m/z*: 287 $[M-H]^-$

(1S, 2S)-2-(4-iodophenyl)cyclopropanecarboxylic acid (10)

Yield: 80%^{1}H NMR (DMSO-d_6) δ (ppm): 12.29 (br s, 1 H, -COO*H*), 7.60 (d, *J*=8.3 Hz, 2 H, aromatic protons), 6.99 (d, *J*=8.3 Hz, 2 H, aromatic protons), 2.41–2.27 (m, 1 H, -C*H* cyclopropane), 1.85–1.71 (m, 1 H, -C*H* cyclopropane), 1.46–1.36 (m, 1 H, -C*H*H cyclopropane), 1.35–1.24 (m, 1 H, -CH*H* cyclopropane); MS (ESI): *m/z*: 287 $[M-H]^-$

***tert*-butyl *N*-[*trans*-2-(4-iodophenyl)cyclopropyl]carbamate (11)**

7.4 g (27 mmol) Diphenyl phosphoryl azide and 4.4 mL (32 mmol) TEA were added to a solution of 7.05 g (24.5 mmol) of *trans*-2-(4-iodophenyl) cyclopropanecarboxylic acid in 150 mL dry *t*-BuOH. After stirring at 90 °C for 20 h the solution was concentrated and the residue was partitioned between 10% aqueous Na_2CO_3 and Et_2O. The combined organic layers were dried over Na_2SO_4, filtered, and concentrated. The crude product was purified by flash

chromatography (hexane/EtOAc 9:1, v:v) giving 5.6 g (62%) of the *tert*-butyl carbamate **11** as white solid. ^{1}H NMR (DMSO-d_6) δ (ppm): 7.67–7.51 (m, 2 H, aromatic protons), 7.25 (br s, 1 H, N*H*COO*t*Bu), 6.98–6.84 (m, 2 H, aromatic protons), 2.57 (br s, 1 H, -C*H* cyclopropane), 1.89–1.74 (m, 1 H, -C*H* cyclopropane), 1.37 (s, 9 H, -COO(CH_3)$_3$), 1.18–0.95 (m, 2 H, -CH_2 cyclopropane); MS (ESI): *m/z*: 260 [MH-100]$^+$.

The following carbamates were prepared according to the procedure for compound **11**:

tert-butyl N-[(1R,2S)-2-(4-iodophenyl)cyclopropyl]carbamate (12)

Yield: 84%. ^{1}H NMR ($CDCl_3$) δ (ppm): 7.62–7.53 (m, 2 H, aromatic protons), 6.96–6.82 (m, 2 H, aromatic protons), 4.93–4.72 (m, 1 H, -N*H*COO*t*Bu), 2.76–2.60 (m, 1 H, -C*H* cyclopropane), 2.05–1.91 (m, 1 H, -C*H* cyclopropane), 1.46 (s, 9 H, -COO(CH_3)$_3$), 1.21–1.07 (m, 2 H, -CH_2 cyclopropane); MS (ESI): *m/z*: 382 [MNa]$^+$. $[\alpha]_D^{20}$ = -74° (c 0.688, MeOH).

***tert*-butyl N-[(1S,2R)- 2-(4-iodophenyl)cyclopropyl]carbamate (13)**

Yield: 81%. ^{1}H NMR ($CDCl_3$) δ (ppm): 7.32–7.22 (m, 2 H, aromatic protons), 7.21–7.09 (m, 3 H, aromatic protons), 4.97–4.65 (m, 1 H, -N*H*COO*t*Bu), 2.85–2.64 (m, 1 H, -C*H* cyclopropane), 2.09–1.99 (m, 1 H-C*H* cyclopropane), 1.47 (s, 9 H, -COO(CH_3)$_3$), 1.23–1.10 (m, 2 H, -CH_2 cyclopropane); MS (ESI): *m/z*: 260 [MH-100]$^+$. $[\alpha]_D^{20}$ = +89.23° (c 1.003, MeOH).

3-(2-Oxooxazolidin-3-yl)benzamide (19e)

A suspension of 0.56 g (2.7 mmol) 3-(2-oxooxazolidin-3-yl)benzoic acid (**18e**) (Enamine) in 15 mL dry CH_2Cl_2 was treated with 0.246 mL (3.38 mmol) thionyl chloride and 2 drops of dry DMF. After stirring at reflux for 2 h, the mixture was cooled down to RT and poured into 4 mL of an aqueous solution of NH_3 (28-30% in water). After 1 h the resulting mixture was filtered off to afford a white solid that was washed with water. The aqueous phases were extracted with CH_2Cl_2, the combined organic layers were dried over Na_2SO_4, filtered and concentrated to give

0.549 g (98%) of the benzamide **19e** as a white solid. **19e** ^{1}H NMR (DMSO-d_6) δ (ppm): 8.01 (br s, 1 H, -CON*H*H), 7.94–7.88 (m, 1 H, aromatic proton), 7.84–7.78 (m, 1 H, aromatic proton), 7.61 (d, *J*=7.8 Hz, 1 H, aromatic proton), 7.52–7.34 (m, 2 H, aromatic proton, -CONH*H*), 4.49–4.39 (m, 2 H, -CH_2O oxazolidinone), 4.14–3.98 (m, 2 H, -CH_2N oxazolidinone); MS (ESI): *m/z*: 207 $[M+H]^+$.

4-(2-Oxooxazolidin-3-yl)benzamide (19f)

4-(2-Oxooxazolidin-3-yl)benzamide (**19f**) was prepared according to the procedure for compound **19e** starting from 4-(2-oxo-1,3-oxazolidin-3-yl)benzoic acid (**18f**, Enamine). Yield: ^{1}H NMR (DMSO-d_6) δ (ppm): 8.01–7.79 (m, 3 H, aromatic protons, -CON*H*H), 7.67–7.53 (m, 2 H, aromatic protons), 7.28 (br s, 1 H, -CONH*H*), 4.44 (t, *J*=7.6 Hz, 2 H, -CH_2O oxazolidinone), 4.08 (t, *J*=7.6 Hz, 2 H, -CH_2N oxazolidinone); MS (ESI): *m/z*: 207 $[M+H]^+$.

4-(1-methyl-4-piperidyl)benzamide (19g)

0.34 g (5.1 mmol) Sodium cyanoborohydride and 0.75 mL acetic acid was added to a mixture of 0.745 g (3.63 mmol) of 4-(1-methyl-4-piperidyl)benzoic acid (**18g**, Fluorochem) and 0.54 mL 37% aqueous formaldehyde in 7.5 mL MeOH. The mixture was stirred for about 30 min, then quenched with water and concentrated. The crude reaction intermediate was taken up with dry CH_2Cl_2 and 0.331 mL (4.54 mmol) thionyl chloride and 2 drops of dry DMF were added. The solution was stirred at reflux for about 2 h, then cooled down to RT, and a further portion of 331 µL (4.538 mmol) thionyl chloride was added. Stirring at reflux was then continued for additional 2 h. For a complete conversion a third portion of 0.331 mL (4.54 mmol) of thionyl chloride was added. After further 2 h at reflux, the mixture was cooled down to RT and poured onto an ice cold solution of 15 mL of aqueous NH_3(28-30%); and the resulting mixture was partitioned between CH_2Cl_2 and an 10% solution of Na_2CO_3 in water. The organic layer was dried over

Na_2SO_4 and concentrated to give 442 mg, (55% from compound **18g**) of benzamide **19g** as a beige solid. ^{1}H NMR (DMSO-d_6) δ (ppm): 7.80 - 7.58 (m, 3 H, -CON*H*H, aromatic protons), 7.11 - 6.85 (m, 3 H, -CONH*H*, aromatic protons), 3.27 - 3.15 (m, 4 H, -CH_2N piperazine), 2.46 - 2.34 (m, 4 H, -CH_2N piperazine), 2.21 (s, 3 H, -NCH_3) MS (ESI): *m/z*: 219 $[M+H]^+$.

_N_-[4-[*trans*-2-aminocyclopropyl]phenyl]-4-(4-methylpiperazin-1-yl)benzamide dihydrochloride (14d)

6 mg (0.03 mmol) CuI, 220 mg (0.613 mmol) of the carbamate **11**, 0.15 mg (0.67 mmol) 4-(4-methylpiperazin-1-yl)benzamide and 0.17 g (1.23 mmol) K_2CO_3 were placed in a vial and charged with nitrogen. 5 mg (0.06 mmol) *N*,*N*'-dimethylethane-1,2-diamine and 2 mL dioxane were added with a syringe, and the vial was heated to 110°C for 20 h. The resulting suspension was allowed to cool down to RT and was then filtered through a silica gel pad eluting with 25 ml of 9:1 CH_2Cl_2/MeOH. The filtrate was concentrated and the residue was purified by chromatography (CH_2Cl_2 to CH_2Cl_2/MeOH 95/5) to give 223 mg (81%) of *N*-[*trans*-2-[4-[[4-(4-methylpiperazin-1-yl)benzoyl]amino]phenyl]cyclopropyl]-carbamate as a white solid. ^{1}H NMR (DMSO-d_6) δ (ppm): 9.86 (s, 1 H, -CON*H*), 7.92–7.77 (m, 2 H, aromatic protons), 7.69–7.57 (m, 2 H, aromatic protons), 7.22 (br s, 1 H, -N*H*COO*t*Bu), 7.08–6.90 (m, 4 H, aromatic protons), 3.31–3.15 (m, 4 H, -CH_2N piperazine), 2.62–2.53 (m, 1 H, -C*H* cyclopropane), 2.47–2.36 (m, 4 H, -CH_2N piperazine), 2.22 (s, 3 H, -NCH_3), 1.90–1.79 (m, 1 H, -C*H* cyclopropane), 1.38 (s, 9 H, -COO(CH_3)$_3$), 1.13–1.02 (m, 2 H, -CH_2 cyclopropane); MS (ESI): *m/z*: 451 $[M+H]^+$.Then, 2 mL of 2 M HCl in Et_2O was added to a solution of 200 mg (0.44 mmol) of *N*-[*trans*-2-[4-[[4-(4-methylpiperazin-1-yl)benzoyl]amino]phenyl]cyclopropyl]carbamate in 3 mL Et_2O/MeOH (2:1, v:v) cooled down to 0°C. After stirring at RT for 20 h the formed precipitate was filtered off and the light yellow solid washed with Et_2O and dried at 40°C under vacuum giving 167 mg (89%)

of *N*-[4-[*trans*-2-aminocyclopropyl]phenyl]-4-(4-methylpiperazin-1-yl)benzamide as its dihydrochloride salt. ^{1}H NMR (DMSO-d_6) δ (ppm): 9.97 (s, 1 H, -N*H*$^+$ CH_3 methyl piperazine), 9.75 (br s, 1 H, -CON*H*), 8.22 (br s, 3 H, -NH_3^+), 7.98–7.83 (m, 2 H, aromatic protons), 7.77–7.63 (m, 2 H, aromatic protons), 7.20–6.98 (m, 4 H, aromatic protons), 4.14–3.93 (m, 2 H, -CH_2N piperazine), 3.60–3.45 (m, 2 H, -CH_2N piperazine), 3.18–2.98 (m, 4 H, -CH_2N piperazine), 2.87 (s, 3 H, -NCH_3), 2.83–2.74 (m, 1 H, -C*H* cyclopropane), 2.27–2.17 (m, 1 H, -C*H* cyclopropane), 1.35–1.27 (m, 1 H, -C*H*H cyclopropane), 1.24–1.14 (m, 1 H, -CH*H* cyclopropane); MS (ESI): *m/z*: 351 [M+H]$^+$.

The following cyclopropylamines were prepared following the procedure for compound **14d** starting from the carbamate **11 (14a-c, 14e-g**), **12** (**15**) or **13** (**16**).

***N*-[4-[*trans*-2-aminocyclopropyl]phenyl]-4-(3-furyl)benzamide hydrochloride(14a)**

Yield: 40% from **11**. ^{1}H NMR (DMSO-d_6) δ (ppm): 10.21 (s, 1 H, -CON*H*), 8.40–8.24 (m, 4 H, -C*H* furan, -NH_3^+), 8.01–7.94 (m, 2 H, aromatic protons), 7.81–7.75 (m, 3 H, aromatic protons), 7.74–7.68 (m, 2 H, aromatic protons), 7.17–7.11 (m, 2 H, aromatic protons), 7.09–7.05 (m, 1 H, -C*H* furan), 2.86–2.74 (m, 1 H, -C*H* cyclopropane), 2.32–2.21 (m, 1 H, -C*H* cyclopropane), 1.40–1.29 (m, 1 H, -C*H*H cyclopropane), 1.25–1.11 (m, 1 H, -CH*H* cyclopropane); MS (ESI): *m/z*: 319 [M+H]$^+$.

Benzyl *N*-[3-[[4-[*trans*-2-aminocyclopropyl]phenyl]carbamoyl]phenyl]carbamate hydrochloride (14b)

Yield: 48% from **11**. ^{1}H NMR (DMSO-d_6) δ (ppm): 10.24 (s, 1 H, -N*H*COO), 9.99 (s, 1 H, -CON*H*), 8.56 (br s, 3 H, -NH_3^+), 8.06–7.02 (m, 13 H, aromatic protons), 5.17 (s, 2 H, -CH_2O), 2.82–2.68 (m, 1 H, -C*H* cyclopropane), 2.38–2.26 (m, 1 H,) -C*H* cyclopropane, 1.45–1.10 (m, 2 H, -CH_2 cyclopropane); MS (ESI): *m/z*: 402 [M+H]$^+$.

***N*-[4-[(*trans*-2-aminocyclopropyl]phenyl]-4-morpholino-benzamide hydrochloride (14c)**

Yield: 21% from **11**. ^{1}H NMR (DMSO-d_6) δ (ppm): 9.93 (s, 1 H, -CON*H*), 8.31 (br s, 3 H, -NH_3^+), 7.93–7.81 (m, 2 H, aromatic protons), 7.74–7.62 (m, 2 H, aromatic protons), 7.17–7.07 (m, 2 H, aromatic protons), 7.05–6.96 (m, 2 H, aromatic protons), 3.79–3.68 (m, 4 H, -CH_2O morpholine), 3.29–3.19 (m, 4 H, -CH_2N morpholine), 2.85–2.71 (m, 1 H, -C*H* cyclopropane), 2.31–2.19 (m, 1 H, -C*H* cyclopropane), 1.40–1.27 (m, 1 H, -C*H*H cyclopropane), 1.23–1.14 (m, 1 H, -CH*H* cyclopropane); MS (ESI): *m/z*: 338 $[M+H]^+$.

***N*-[4-[*trans*-2-aminocyclopropyl]phenyl]-3-(2-oxooxazolidin-3-yl)benzamide hydrochloride (14e)**

Yield: 49% from **11**. ^{1}H NMR (DMSO-d_6) δ (ppm): 10.29 (s, 1 H, -CON*H*), 8.31 (br s, 3 H, -NH_3^+), 8.07–8.00 (m, 1 H, aromatic proton), 7.84–7.77 (m, 1 H, aromatic proton), 7.73–7.66 (m, 3 H, aromatic protons), 7.59–7.50 (m, 1 H, aromatic proton), 7.19–7.12 (m, 2 H, aromatic protons), 4.51–4.43 (m, 2 H, -CH_2O oxazolidinone), 4.20–4.08 (m, 2 H, -CH_2N oxazolidinone), 2.87–2.75 (m, 1 H, -C*H* cyclopropane), 2.32–2.21 (m, 1 H, -C*H* cyclopropane), 1.39–1.29 (m, 1 H, -C*H*H cyclopropane), 1.27–1.15 (m, 1 H, -CH*H* cyclopropane); MS (ESI): *m/z*: 338 $[M+H]^+$.

***N*-[4-[*trans*-2-aminocyclopropyl]phenyl]-4-(2-oxooxazolidin-3-yl)benzamide trifluoroacetate (14f)**

Yield: 10% from **11** and after purification of the final product by preparative HPLC. ^{1}H NMR (DMSO-d_6) δ (ppm): 10.16 (s, 1 H, -CON*H*), 8.12 (br s, 3 H, -NH_3^+), 8.02–7.96 (m, 2 H, aromatic protons), 7.74–7.66 (m, 4 H, aromatic protons), 7.18–7.08 (m, 2 H, aromatic protons), 4.55–4.40 (m, 2 H, -CH_2O oxazolidinone), 4.20–4.02 (m, 2 H, -CH_2N oxazolidinone), 2.85–2.74 (m, 1 H, -C*H* cyclopropane), 2.31–2.15 (m, 1 H, -C*H*H cyclopropane), 1.36–1.13 (m, 2 H, -CH*H* cyclopropane); MS (ESI): *m/z*: 338 $[M+H]^+$.

***N*-[4-[*trans*-2-aminocyclopropyl]phenyl]-4-(1-methyl-4-piperidyl)benzamide trifluoroacetate (14g)**

Yield: 10% from **11** and after purification of the final product by preparative HPLC. ^{1}H NMR (DMSO-d_6) δ (ppm): 10.17 (s, 1 H, -CON*H*), 9.39 (br s, 1 H, -N*H*$^+$CH3 piperidine), 8.23 (br s, 3 H, -NH_3^+), 7.98–7.87 (m, 2 H, aromatic protons), 7.73–7.61 (m, 2 H, aromatic protons), 7.48–7.31 (m, 2 H, aromatic protons), 7.19–7.09 (m, 2 H, aromatic protons), 3.61–3.45 (m, 2 H, -CH_2N piperidine), 3.14–2.99 (m, 2 H, -CH_2N piperidine), 2.94–2.75 (m, 5 H, -NCH_3, -C*H* piperidine, -C*H* cyclopropane), 2.30–2.19 (m, 1 H, -C*H* cyclopropane), 2.12–1.98 (m, 2 H, -CH_2 piperidine), 1.93–1.78 (m, 2 H, -CH_2 piperidine), 1.36–1.28 (m, 1 H, -C*H*H cyclopropane), 1.23–1.14 (m, 1 H, -CH*H* cyclopropane); MS (ESI): *m/z*: 350 [M+H]$^+$.

N-[4-[(1S,2R)-2-aminocyclopropyl]phenyl]-4-(4-methylpiperazin-1-yl)benzamide dihydrochloride (15)

^{1}H NMR (DMSO-d_6) δ (ppm): 10.85 (br. s., 1 H, -N*H*$^+$CH3 piperazine), 10.00 (s, 1 H, -CON*H*), 8.44 (br. s, 3 H, -NH_3^+), 7.95 - 7.85 (m, 2 H, aromatic protons), 7.74 - 7.65 (m, 2 H, aromatic protons), 7.10 (dd, J = 9.0, 12.5 Hz, 4 H, aromatic protons), 4.07 - 3.96 (m, 2 H, -CH_2N piperazine), 3.54 - 3.43 (m, 2 H, -CH_2N piperazine), 3.25 - 3.07 (m, 4 H, -CH_2N piperazine), 2.86 - 2.70 (m, 4 H, -NCH_3, -C*H* cyclopropane), 2.33 - 2.23 (m, 1 H, -C*H* cyclopropane), 1.41 - 1.30 (m, 1 H, -C*H*H cyclopropane), 1.22 - 1.11 (m, 1 H, -CH*H* cyclopropane); MS (ESI): *m/z*: 351 [M+H]$^+$. $[\alpha]_D^{20}$ = -46.48° (c 0.00236, DMSO).

***N*-[4-[(1R,2S)-2-aminocyclopropyl]phenyl]-4-(4-methylpiperazin-1-yl)benzamide dihydrochloride (16):**

^{1}H NMR (DMSO-d_6) δ (ppm): 11.00 (br. s., 1 H, -N*H*$^+$CH3 piperazine), 10.01 (s, 1 H, -CON*H*), 8.48 (br. s, 3 H, -NH_3^+), 7.97 - 7.85 (m, 2 H, aromatic protons), 7.74 - 7.63 (m, 2 H, aromatic

protons), 7.17 - 7.01 (m, 4 H, aromatic protons), 4.08 - 3.95 (m, 2 H, -C*H*$_2$N piperazine), 3.54 - 3.42 (m, 2 H, -C*H*$_2$N piperazine), 3.27 - 3.03 (m, 4 H, -C*H*$_2$N piperazine), 2.87 - 2.67 (m, 4 H, -NC*H*$_3$, -C*H* cyclopropane), 2.36 - 2.23 (m, 1 H, -C*H* cyclopropane), 1.43 - 1.30 (m, 1 H, -C*H*H cyclopropane), 1.22 - 1.09 (m, 1 H, -CH*H* cyclopropane); MS (ESI): *m/z*: 351 $[M+H]^+$. $[\alpha]_D^{20}$ = +41.21° (c 0.00236, DMSO).

***tert*-Butyl 4-(4-methylpiperazin-1-yl)-3-nitrobenzoate (19j)**

A suspension of 2.0 g (7.8 mmol) *tert* butyl 4-chloro-3-nitro-benzoate, 3.22 g (23.3 mmol) of dry K_2CO_3) and 2.58 mL (23.3 mmol) of *N*-methylpiperazine was stirred in 10 mL of dry DMF at 90°C for 5 h in a sealed tube. Then, the reaction mixture was quenched with water and extracted with EtOAc. The combined organic phases were washed with brine, dried over Na_2SO_4, concentrated and the residue was purified on silica gel (eluent: EtOAc) and recrystallized from toluene to obtain 2.3 g (92%) of intermediate **19j** as a yellow solid. ^{1}H NMR ($CDCl_3$, 400 MHz) δ 8.37 (s, 1H, aromatic proton), 8.03-8.06 (d, 1H, aromatic proton), 7.07-7.10 (d, 1H, aromatic proton), 3.20 (t, 4H, -PhN(C*H*$_2$)$_2$), 2.58 (t, 4H, -CH$_3$N(C*H*$_2$)$_2$), 2.38 (s, 3H, -NC*H*$_3$), 1.61 (s, 9H, -COOC(C*H*$_3$)$_3$) ppm; ^{13}C NMR ($CDCl_3$, 100 MHz) δ 164.9, 147.8, 137.2, 135.8, 134.0, 119.3, 115.8, 82.6, 57.7 (2C), 51.9 (2C), 47.0, 28.9 (3C) ppm; MS (EI) *m/z*: 321.17 $[M]^+$; m.p. 138-140°C. The following *tert*-butyl benzoates were prepared starting from *tert* butyl 3-chloro-4-nitro-benzoate and morpholine (**19i**) or *tert* butyl 4-chloro-3-nitro-benzoate and piperidine (**19k**) or morpholine (**19h**) according to the procedure for intermediate **19j**.

***tert*-butyl 4-morpholino-3-nitro-benzoate (19h)**

Yield: 85%. ^{1}H NMR ($CDCl_3$, 400 MHz) δ 8.38-8.39 (d, 1H, aromatic proton), 8.06-8.08 (dd, 1H, aromatic proton), 7.08-7.10 (d, 1H, aromatic proton), 3.87 (t, 4H, -O(C*H*$_2$)$_2$), 3.16 (t, 4H, -N(CH$_2$)$_2$), 1.61 (s, 9H, -COOC(C*H*$_3$)$_3$) ppm; ^{13}C NMR ($CDCl_3$, 100 MHz) δ 165.1, 148.7, 134.9,

134.8, 131.0, 122.5, 120.1, 81.5, 66.9 (2C), 51.3 (2C), 28.2 (3C) ppm; MS (EI) *m/z*: 308.14 $[M]^+$; m.p. 149-151°C.

***tert*-butyl 3-morpholino-4-nitro-benzoate (19i)**

Yield: 87 %. ^{1}H NMR ($CDCl_3$, 400 MHz) δ 7.79 (d, 1H, aromatic proton), 7.76 (d, 1H, aromatic proton), 7.65-7.67 (dd, 1H, aromatic proton), 3.86 (t, 4H, -O(CH_2)$_2$), 3.10 (t, 4H, -N(CH_2)$_2$), 1.63 (s, 9H, -COOC(CH_3)$_3$) ppm; ^{13}C NMR ($CDCl_3$, 100 MHz) δ 165.1, 142.8, 138.4, 130.9, 127.1, 121.7, 120.1, 81.5, 66.7 (2C), 51.4 (2C), 28.2 (3C) ppm; MS (EI) *m/z*: 308.14 $[M]^+$; m.p. 57-60°C.

***tert*-butyl 4-(1-piperidyl)-3-nitro-benzoate (19k)**

Yield: 88%. ^{1}H NMR ($CDCl_3$, 400 MHz) δ 8.38 (d, 1H, aromatic proton), 7.98-8.00 (dd, 1H, aromatic proton), 7.07-7.08 (d, 1H, aromatic proton), 2.89 (t, 4H, -N(CH_2)$_2$), 1.62-1.64 (m, 6H, piperidine protons), 1.54 (s, 9H, -COOC(CH_3)$_3$) ppm; ^{13}C NMR ($CDCl_3$, 100 MHz) δ 165.1, 148.7, 134.9, 134.8, 131.0, 122.5, 120.1, 81.5, 52.6 (2C), 28.2 (3C), 26.1 (2C), 24.0 ppm; MS (EI) *m/z*: 306.16 $[M]^+$; m.p. 144-146°C.

***tert*-Butyl 3-amino-4-(4-methylpiperazin-1-yl)benzoate (20j)**

A suspension of 0.80 g (2.5 mmol) of the *tert*-butyl nitrobenzoate **19j** in 30 mL MeOH and 0.13 g (0.12 mmol) of 10% palladium on carbon were placed in a Parr apparatus and was hydrogenated at 50 psi and 25°C for 5 h. The palladium was then filtered off and the MeOH was evaporated to afford an oily residue that was first purified on silica gel (eluent: $CHCl_3$/MeOH, 10:1, v:v) and then recrystallized from cyclohexane to provide 0.29 g (65%) of the *tert*-butyl 4-amino-benzoate **20j** as a yellow solid. ^{1}H NMR ($CDCl_3$, 400 MHz) δ 7.41-7.43 (dd, 1H, aromatic proton), 7.36 (d, 1H, aromatic proton), 6.99-7.00 (d, 1H, aromatic proton), 3.96 (s, 2H, Ph(NH_2)), 2.98 (t, 4H, -PhN(CH_2)$_2$), 2.61 (t, 4H, -CH_3N(CH_2)$_2$), 2.38 (s, 3H, -N(CH_3)),

1.58 (s, 9H,-COOC(C*H*$_3$)$_3$) ppm; ^{13}C NMR ($CDCl_3$, 100 MHz) δ 165.1, 141.5, 137.7, 124.5 (2C), 119.9, 117.3, 81.5, 53.2 (2C), 50.0 (2C), 44.7, 28.2 (3C) ppm; MS (EI) *m/z*: 291.19 $[M]^+$; m.p. 114-116°C.

The following *tert*-butyl benzoates were prepared starting from the *tert* butyl benzoates **19h**, **19i** or **19k** according to the procedure for intermediate **20j**.

***tert*-butyl 4-morpholino-3-amino-benzoate (20h)**

Yield: 73%. $_1$H NMR ($CDCl_3$, 400 MHz) δ 7.42-7.45 (d, 1H, aromatic proton), 7.38 (s, 1H, aromatic proton), 6.98-7.02 (d, 1H, aromatic proton), 4.0 (br s, 2H, -PhN*H*$_2$), 3.88 (t, 4H, -O(C*H*$_2$)$_2$), 2.98 (t, 4H, -N(C*H*$_2$)$_2$), 1.61 (s, 9H, -COOC(C*H*$_3$)$_3$) ppm; ^{13}C NMR ($CDCl_3$, 100 MHz) δ 164.7, 142.2, 134.4, 120.7, 120.5, 115.4, 115.0, 81.7, 66.3 (2C), 53.4 (2C), 28.8 (3C) ppm; MS (EI) *m/z*: 278.16 $[M]^+$; m.p. 126-128°C.

***tert*-butyl 3-morpholino-4-amino-benzoate (20i)**

Yield: 84%. ^{1}H NMR (CDCl*3*, 400 MHz) δ 7.68 (d, 1H, aromatic proton), 7.63 (dd, 1H, aromatic proton), 6.69-6.71 (d, 2H, aromatic proton), 4.39 (br s, 2H, -PhN*H*$_2$), 3.87 (t, 4H, -O(C*H*$_2$)$_2$), 2.93(t, 4H, -N(C*H*$_2$)$_2$), 1.59 (s, 9H, -COOC(C*H*$_3$)$_3$) ppm; ^{13}C NMR ($CDCl_3$, 100 MHz) δ 165.1, 140.1, 139.2, 123.8, 123.3, 119.2, 115.4, 81.5, 66.6 (2C), 50.5 (2C), 28.2 (3C) ppm; MS (EI) *m/z*: 278.16; m.p. 136-138°C.

***tert*-butyl 4-(1-piperidyl)-3-amino-benzoate (20k)**

Yield: 67%. ^{1}H NMR ($CDCl_3$, 400 MHz) δ 7.11-7.13 (dd, 1H, aromatic proton), 6.81 (d, 1H, aromatic proton), 6.58-6.60 (d, 1H, aromatic proton), 4.35 (s, 2H, -N*H*$_2$), 2.96 (t, 4H, piperidine proton), 1.77 (m, 4H, piperidine proton), 1.63 (m, 2H, piperidine proton), 1.54 (s, 9H, -COOC(C*H*$_3$)$_3$) ppm; ^{13}C NMR ($CDCl_3$, 100 MHz) δ 165.1, 141.5, 137.7, 124.6, 124.5, 120.0,

117.3, 81.5, 51.0 (2C), 28.2 (3C), 25.6 (2C), 24.0 ppm; MS (EI) *m/z*: 276.18 $[M]^+$; m.p. 115-117°C.

***tert*-Butyl 3-(benzyloxycarbonylamino)-4-(4-methylpiperazin-1-yl)benzoate (21j)**

Benzyl chloroformate (2.1 mmol, 0.3 mL) was slowly added at 0°C to a solution of 0.50 g (1.72 mmol) of *tert*-butyl 4-amino-3-(4-methylpiperazin-1-yl)benzoate (**20j**) 1in 10 mL of THF and 0.29 mL (2.1 mmol) of TEA. After stirring at RT for 1.5 h the solution was then quenched with water (20 mL) and extracted with CH_2Cl_2 (3 x 20 mL). The organic phases were washed with brine, dried over Na_2SO_4 and concentrated to afford a residue that was purified on silica gel (eluent EtOAc/$CHCl_3$, 1:1, v:v) providing 0.53 g (65%) of the *tert*-butyl benzoate **21j**. ^{1}H NMR ($CDCl_3$, 400 MHz) δ 8.69 (br s, 1H, -PhN*H*COO), 7.69-7.71 (m, 2H, aromatic proton), 7.37-7.47 (m, 5H, -C*H*$_2$Ph), 7.15-7.17 (d, 1H, aromatic proton), 5.28 (s, 2H, -COOC*H*$_2$Ph), 2.92 (t, 4H, -PhN(C*H*$_2$)$_2$), 2.61 (t, 4H, CH_3N(C*H*$_2$)$_2$), 2.20 (s, 3H, -N(C*H*$_3$)), 1.60 (s, 9H, -COOC(C*H*$_3$)$_3$) ppm;^{13}C NMR ($CDCl_3$, 100 MHz) δ 165.1, 155.9, 144.2, 136.3, 130.3, 128.3 (2C), 128.1 (2C), 127.9, 124.4, 124.0, 120.9, 118.1, 81.5, 67.0, 53.2 (2C), 50.0 (2C), 44.7, 28.2 (3C) ppm; MS (EI) *m/z*: 425.23 $[M]^+$.

The following *tert*-butyl benzoates were prepared starting from the *tert* butyl benzoates **20h**, **20i** or **20k** according to the procedure for intermediate **21j**.

***tert*-butyl 4-morpholino-3-(benzyloxycarbonylamino)-benzoate (21h)**

Yield: 71%. ^{1}H NMR ($CDCl_3$, 400 MHz) δ 8.71 (br s, 1H, -PhN*H*COO), 7.71-7.73 (m, 2H, aromatic proton), 7.38-7.47 (m, 5H, -C*H*$_2$Ph), 7.15-7.17 (d, 1H, aromatic proton), 5.27 (s, 2H, -COOC*H*$_2$Ph), 3.88 (t, 4H, -O(C*H*$_2$)$_2$), 2.89 (t, 4H, -N(C*H*$_2$)$_2$), 1.60 (s, 9H, -COOC(C*H*$_3$)$_3$) ppm;^{13}C NMR ($CDCl_3$, 100 MHz) δ 165.1, 155.9, 144.2, 136.3, 130.3, 128.3 (2C), 128.1 (2C), 128.0, 124.4, 124.0, 120.9, 118.1, 81.5, 67.0, 66.6 (2C), 50.5 (2C), 28.2 (3C) ppm; MS (EI) *m/z*:

425.23 $[M]^+$.

***tert*-butyl 3-morpholino-4-(benzyloxycarbonylamino)-benzoate (21i)**

Yield: 73%. ^{1}H NMR ($CDCl_3$, 400 MHz) δ 8.20 (d, 1H, aromatic proton), 8.15 (br s, 1H, -Ph(NH)COO), 7.81-7.83 (m, 2H, aromatic protons), 7.38-7.45 (m, 5H, -CH_2(Ph)), 5.26 (s, 2H, -COO(CH_2)Ph), 3.88 (t, 4H, -O(CH_2)$_2$), 2.89 (t, 4H, -N(CH_2)$_2$), 1.61 (s, 9H, -COOC(CH_3)$_3$)ppm; ^{13}C NMR ($CDCl_3$, 100 MHz) δ 165.1, 155.9, 138.8, 136.3, 128.8, 128.3 (2C), 128.1 (2C), 127.9, 125.1, 122.4, 120.8, 118.6, 81.5, 67.0, 66.6 (2C), 50.5 (2C), 28.2 (3C) ppm; MS (EI) *m/z*: 425.23 $[M]^+$.

***tert*-butyl 4-(1-piperidyl)-3-(benzyloxycarbonylamino)-benzoate (21k)**

Yield: 68%. ^{1}H NMR ($CDCl_3$, 400 MHz) δ 8.08-8.11 (dd, 1H, aromatic proton), 7.86-7.87 (d, 1H, aromatic proton), 7.33 (m, 5H, aromatic protons), 7.03 (d, 1H, aromatic proton), 6.80 (s, 1H, -CON*H*Ph), 5.10 (s, 2H, -COOC*H*$_2$Ph), 2.96 (t, 4H, piperidine protons), 1.77 (m, 4H, piperidine protons), 1.63 (m, 2H, piperidine protons), 1.54 (s, 9H, -COOC(C*H*$_3$)$_3$) ppm; ^{13}C NMR ($CDCl_3$, 100 MHz) δ 165.1, 155.8, 144.2, 136.3, 130.3, 128.3 (2C), 128.1 (2C), 127.9, 124.4, 124.0, 120.9, 118.1, 81.5, 67.0, 51.0 (2C), 28.2 (3C), 25.6 (2C), 23.9 ppm; MS (EI) *m/z*: 410.22 $[M]^+$.

3-(benzyloxycarbonylamino)-4-(4-methylpiperazin-1-yl)benzoic acid (18j)

A solution of 0.20 g (0.47 mmol) of *tert*-butyl benzoate **21j**, and 0.72 mL (9.4 mmol) of TFA in 5 mL of dry CH_2Cl_2 was stirred at RT overnight. The solvent was then removed and the resulting solid was first triturated with 10 mL Et_2O and then crystallized from acetonitrile to give 0.13 g (76%) of the benzoic acid **18j** as a colorless solid. ^{1}H NMR (DMSO-d_6, 400 MHz) δ 12.84 (br s, 1H, -COO*H*), 9.85 (br s, 1H, -PhN*H*COO), 8.36 (s, 1H, aromatic proton), 7.66-7.68 (d, 1H, aromatic proton), 7.40-7.46 (m, 3H, aromatic protons), 7.36-7.38 (d, 2H, aromatic protons), 7.22-7.25 (d, 1H, aromatic proton), 5.22 (s, 2H, -COOC*H*$_2$Ph), 3.20 (t, 4H, -PhN(C*H*$_2$)$_2$), 3.08 (t, 4H,

$CH_3N(CH_2)_2$), 2.86 (s, 3H, -N(CH_3)) ppm; ^{13}C NMR (DMSO- d_6, 100 MHz) δ 167.6, 155.8, 145.2, 136.3, 129.3, 128.3 (2C), 128.1 (2C), 127.9, 125.2, 125.1, 119.7, 118.2, 67.0, 53.2 (2C), 50.0 (2C), 44.7 ppm; MS (EI) *m/z*: 369.17 $[M]^+$; m.p. 205-207°C.

The following *tert*-butyl benzoates were prepared starting from the *tert* butyl benzoates **21h**, **21i** or **21k** according to the procedure for intermediate **18j**.

4-morpholino-3-(benzyloxycarbonylamino)-benzoic acid (18h)

Yield: 83%. ^{1}H NMR (DMSO-d_6, 400 MHz) δ 12.88 (br s, 1H, -COO*H*), 9.72 (br s, 1H, -NH^+), 8.76 (br s, 1H, -N*H*COOCH_2Ph), 8.04-8.06 (d, 1H, aromatic proton), 7.75-7.77 (d, 1H, aromatic proton), 7.70 (s, 1H, aromatic proton), 7.36-7.47 (m, 5H, -CH_2*Ph*), 5.23 (s, 2H, -NHCOOCH_2Ph), 3.46-3.48 (t, 4H, -PhN(CH_2)$_2$), 2.99-3.12 (m, 4H, -$CH_3N(CH_2)_2$), 2.87 (s, 3H, -NCH_3) ppm; ^{13}C NMR (DMSO-d_6, 400 MHz) δ 166.8, 154.1, 142.7, 136.3, 128.8 (2C), 127.5, 127.3 (2C), 126.2, 124.6, 122.7, 120.4, 112.5, 66.9, 57.2 (2C), 52.4 (2C), 46.7 ppm; MS (EI) *m/z*: 356.14 $[M]^+$; m.p. 234-236°C.

3-morpholino-4-(benzyloxycarbonylamino)-benzoic acid (18i)

Yield: 88%. ^{1}H NMR (DMSO-d_6, 400 MHz) δ 12.81 (br s, 1H, -COO*H*), 8.61 (s, 1H, PhN*H*COO), 7.96-7.98 (d, 1H, aromatic proton), 7.71-7.73 (m, 2H, aromatic proton), 7.33-7.46 (m, 5H, -CH_2Ph), 5.22 (s, 2H, -COOCH_2Ph), 3.77 (t, 4H, -O(CH_2)$_2$), 2.81 (t, 4H, -N(CH_2)$_2$) ppm; ^{13}C NMR (DMSO-d_6, 100 MHz) δ 167.6, 155.8, 138.7, 136.3, 130.9, 128.3 (2C), 128.1 (2C), 127.9, 126.7, 122.14, 121.0, 116.2, 67.0, 66.6 (2C), 50.5 (2C) ppm; MS (EI) *m/z*: 369.16 $[M]^+$; m.p. 218-220°C.

4-(1-piperidyl)-3-(benzyloxycarbonylamino)-benzoic acid (18k)

Yield: 86%. ^{1}H NMR (DMSO-d_6, 400 MHz) δ 12.99 (s, 1 H, -COO*H*), 9.88 (s, 1H, -CON*H*Ph), 8.38 (d, 1H, aromatic proton), 8.15-8.17 (dd,1H, aromatic proton), 7.40-7.41 (d, 1H, aromatic

proton), 7.29-7.36 (m, 5H, aromatic protons), 4.87 (s, 2H, -COOC*H*$_2$Ph), 2.99 (t, 4H, piperidine protons), 1.77 (m, 4H, piperidine protons), 1.59 (m, 2H, piperidine protons) ppm; ^{13}C NMR (DMSO-*d*$_6$, 100 MHz) δ 167.6, 155.9, 145.2, 136.3, 129.3, 128.3 (2C), 128.1 (2C), 127.9, 125.2, 125.1, 119.7, 118.2, 67.0, 51.0 (2C), 25.6 (2C), 24.0 ppm; MS (EI) *m/z*: 354.15 $[M]^+$; m.p. 214-216°C.

Benzyl *N*-[5-[[4-[*trans*-2-aminocyclopropyl]phenyl]carbamoyl]-2-(4-methylpiperazin-1-yl)phenyl]carbamate dihydrochloride (14j) 0.15 mL (1.08 mmol) TEA and 0.17 g (0.32 mmol) PyBop were added to a solution of 0.10 g (0.27 mmol) of the benzoic acid **18j**, in dry DMF under nitrogen atmosphere, and the resulting mixture was stirred at RT for 45 min. 0.067 g (2.71 mmol) of *tert*-butyl *N*-[*trans*-2-(4-aminophenyl)cyclopropyl]carbamate (**17**)[48] was added under N_2 atmosphere and the reaction was continued overnight, then quenched with water (20 mL) and the product was extracted with CH_2Cl_2 (3 x 20 mL). The combined organic phases were washed with brine, dried over Na_2SO_4 and concentrated to furnish a residue that was purified by chromatography on silica gel (eluent: EtOAc/$CHCl_3$, 1:1, v:v) giving benzyl *N*-[5-[[4-[*trans*-2-(*tert*-butoxycarbonylamino)cyclopropyl]phenyl]carbamoyl]-2-(4-methylpiperazin-1-yl)phenyl]carbamate. Yield: 68%. ^{1}H NMR ($CDCl_3$, 400 MHz) δ 11.12 (br s, 1H, -N*H*$^+$), 10.27 (br s, 1H, -PhCON*H*), 8.74 (br s, 1H, -N*H*COOCH$_2$Ph), 8.01-8.03 (d, 1H, aromatic proton), 7.79-7.86 (m, 2H, aromatic protons), 7.70-7.72 (d, 2H, aromatic protons), 7.34-7.48 (m, 5H, aromatic protons), 7.13-7.16 (d, 2H, aromatic protons), 5.23 (s, 2H, -NHCOOC*H*$_2$Ph), 4.89 (br s, 1H, -N*H*COOC(CH$_3$)$_3$), 3.32-3.38 (m, 4H, -NC*H*$_3$ and -PhC*H*), 3.15 (m, 4H, -PhN(C*H*$_2$)$_2$), 2.80 (m, 4H, -CH$_3$N(C*H*$_2$)$_2$), 2.31 (m, 1H, -C*H*NH$_2$), 1.50 (s, 9H, -C(C*H*$_3$)$_3$), 1.37 (m, 1H, -C*H*H cyclopropane), 1.18 (m, 1H, -CH*H* cyclopropane) ppm; ^{13}C NMR ($CDCl_3$, 100 MHz) δ 164.9, 155.8, 153.7, 143.3, 137.5, 136.4, 134.5, 130.8, 129.3 (2C), 127.9, 127.6 (2C), 125.3 (2C), 124.5,

122.6, 121.6 (2C), 119.5, 110.3, 79.8, 66.5, 57.4 (2C), 52.3 (2C), 46.8, 32.7, 28.6 (3C), 23.1, 14.5 ppm; MS (EI) *m/z*: 599.31 $[M]^+$. MS (EI) *m/z*: 599.31 $[M]^+$. Then, the Boc protection group was removed by stirring a solution of 0.06 g (0.1 mmol) of benzyl *N*-[5-[[4-[*trans*-2-(*tert*-butoxycarbonylamino)cyclopropyl]-phenyl]carbamoyl]-2-(4-methylpiperazin-1-yl)phenyl]carbamate in tetrahydrofuran (5 mL) and 0.5 mL of 4 M HCl in 1,4-dioxane was stirred at RT overnight. The formed solid was then off and washed with Et_2O (3 x 5 mL) to afford the cyclopropylamine **14j** as a colorless solid (79%). ^{1}H NMR (DMSO-d_6, 400 MHz) δ 11.12 (br s, 1H, -N*H*$^+$), 10.27 (br s, 1H, -PhCON*H*), 8.74 (br s, 1H, -N*H*COOCH$_2$Ph), 8.56 (br s, 3H, -NH_3^+), 8.01-8.03 (d, 1H, aromatic proton), 7.79-7.86 (m, 2H, aromatic protons), 7.70-7.72 (d, 2H, aromatic protons), 7.30-7.48 (m, 5H, aromatic protons), 7.15-7.18 (d, 2H, aromatic protons), 5.23 (s, 2H, -NHCOOCH_2Ph), 3.33 (s, 3H, -NCH_3), 3.15 (m, 4H, -PhN(CH_2)$_2$), 2.83 (t, 4H, -CH$_3$N(CH_2)$_2$), 2.34 (m, 1H, -C*H*NH$_2$), 1.39 (m, 1H, -CH*H* cyclopropane), 1.20 (m, 1H, C*H*H cyclopropane) ppm; ^{13}C NMR (DMSO-d_6, 100 MHz) δ 164.8, 153.8, 146.4, 137.3, 136.3, 134.5, 129.0 (2C), 127.9, 127.4 (2C), 125.9, 125.5 (2C), 123.9, 121.3 (2C), 121.0, 118.2, 114.7, 66.8, 57.3 (2C), 52.1 (2C), 46.7, 34.4, 25.6, 17.3 ppm; MS (ESI) *m/z*: 500 ($[M+H]^+$).

The following *tert*-butyl benzoates were prepared starting from the *tert* butyl benzoates **18h**, **18i** or **18k** according to the procedure for compound **14j**.

Benzyl *N*-[5-[[4-[*trans*-2-aminocyclopropyl]phenyl]carbamoyl]-2-morpholino-phenyl]carbamate hydrochloride (14h)

Yield: 77%**.** ^{1}H NMR (DMSO-d_6, 400 MHz) δ 11.13 (br s, 1H, -N*H*$^+$), 10.30 (br s, 1H, -PhCON*H*), 8.75 (br s, 1H, -N*H*COOCH$_2$Ph), 8.58 (br s, 3H, -NH_3^+), 8.03-8.05 (d, 1H, aromatic proton), 7.79-7.86 (m, 2H, aromatic protons), 7.71-7.73 (d, 2H, aromatic protons), 7.32-7.46 (m, 5H, aromatic protons), 7.15-7.18 (d, 2H, aromatic protons), 5.27 (s, 2H, -NHCOOCH_2Ph), 3.88

(m, 4H, -O(CH_2)$_2$), 2.89 (t, 4H, -N(CH_2)$_2$), 2.33 (m, 1H, -CHNH$_2$), 1.38 (m, 1H, -CHH cyclopropane), 1.21 (m, 1H, -CHH cyclopropane) ppm; ^{13}C NMR (DMSO-d$_6$, 100 MHz) δ 166.0, 155.8, 144.7, 140.3, 136.4, 136.3, 128.9, 128.6, 128.3 (2C), 128.1 (2C), 127.9, 126.3 (2C), 124.7, 122.4 (2C), 120.2, 117.5, 67.0, 66.6 (2C), 50.5 (2C), 36.7, 26.9, 19.5 ppm; MS (ESI) *m/z*: 487 ([M+H]$^+$).

Yield: 77%**.** ^{1}H NMR (DMSO-d$_6$, 400 MHz) δ ^{13}C NMR (DMSO-d$_6$, 100 MHz) δ

Benzyl *N*-[4-[[4-[*trans*-2-aminocyclopropyl]phenyl]carbamoyl]-2-morpholino-phenyl]carbamate hydrochloride (14i)

Yield: 78%**.** ^{1}H NMR (DMSO-d$_6$, 400 MHz) δ 10.15 (br s, 1H, -PhCONH), 8.61 (br s, 1H, -NHCOOCH$_2$Ph), 8.47 (br s, 3H, -NH_3^+), 7.94-8.02 (m, 2H, aromatic protons), 7.74-7.83 (m, 3H, aromatic protons), 7.69-7.71 (d, 1H, aromatic proton), 7.31-7.46 (m, 6H, aromatic protons), 7.14-7.16 (d, 1H, aromatic proton), 5.22 (s, 2H, -NHCOOCH_2Ph), 3.79 (m, 4H, -O(CH_2)$_2$), 2.88 (t, 4H, -N(CH_2)$_2$), 2.33 (m, 1H, -CHNH$_2$), 1.38 (m, 1H, -CHH cyclopropane), 1.22 (m, 1H, -CHH cyclopropane) ppm; ^{13}C NMR (DMSO-d$_6$, 100 MHz) δ 164.8, 153.8, 143.1, 137.3, 136.0, 134.3, 130.8, 128.8 (2C), 127.6, 127.3 (2C), 125.3 (2C), 124.2, 122.7, 121.1 (2C), 119.1, 110.2, 66.9, 66.5 (2C), 53.3 (2C), 34.4, 25.6, 17.4 ppm; MS (EI) *m/z*: 486.23 [M]$^+$.

Benzyl *N*-[5-[[4-[*trans*-2-aminocyclopropyl]phenyl]carbamoyl]-2-(1-piperidyl)phenyl]carbamate hydrochloride (14k)

Yield: 86%**.** ^{1}H NMR (DMSO-d$_6$, 400 MHz) δ 11.12 (br s, 1H, -NH^+), 10.30 (br s, 1H, -PhCONH), 8.74 (br s, 1H, -NHCOOCH$_2$Ph), 8.56 (br s, 3H, -NH_3^+), 8.02-8.04 (d, 1H, aromatic proton), 7.79-7.86 (m, 2H, aromatic protons), 7.68-7.70 (d, 2H, aromatic protons), 7.32-7.46 (m, 5H, aromatic protons), 7.14-7.17 (d, 2H, aromatic protons), 5.23 (s, 2H, -NHCOOCH_2Ph), 3.32-

3.36 (m, 1H, -PhC*H*), 3.0 (t, 4H, --N(CH_2)$_2$), 2.34 (m, 1H, -C*H*NH_2), 1.52-1.59 (m, 6H, piperidine protons), 1.39 (m, 1H, -CH*H* cyclopropane), 1.20 (m, 1H, -C*H*H cyclopropane) ppm; ^{13}C NMR (DMSO-d_6, 100 MHz) δ 164.8, 153.9, 146.5, 137.3, 136.2, 134.5, 128.9 (2C), 127.7, 127.5 (2C), 125.9, 125.4 (2C), 124.0, 121.3 (2C), 120.8, 118.5, 114.8, 66.8, 54.7 (2C), 34.4, 25.7, 25.5 (2C), 24.5, 17.2 ppm; MS (ESI) *m/z*: 485 ([M+H]$^+$).

Biological evaluation.

KDM1A (LSD1) Enzyme Inhibition Assay

The KDM1A (LSD1) enzyme inhibition assay was performed as described previously. [69]

Bioluminescent-Coupled Assay for Monoamine oxidases (MAO Glo Assay)

The MAO Glo Assay from Promega (cat. V1402, Promega, Madison, WI) was performed as described previously.[69]

Cell studies (Transcriptional assay)

The transcriptional assay was performed as described previously.[69]

Cell studies (Clonogenic assay)

Murine acute myeloid leukemia blast

Murine acute myeloid leukemia blasts were recovered from spleen of acute promyelocytic leukemic mice sacrificed once that the spleen was completely blast infiltrated. Specifically, the model was previously characterized and obtained by injection in 129sv mice of lineage-depleted cells from 129sv mice purified and transduced with PML-RARA-expressing retroviral vector[52]. One million of leukemic blast cells (from 129sv mice) injected intravenously into non-irradiated syngenic recipients are able to induce leukemia development leading to mice death 21 days after blast injection.

For the clonogenic assay, murine Acute Myeloid Leukemic cells (20,000 cells) originated from spleen of leukemic mice were seeded in duplicate in methylcellulose medium (MethoCultTM GF M3434, Stem Cell Technology, Vancouver, BC, Canada) in the presence of the compounds at the fixed concentration of 0.25 μM. After 7 days, colonies - were counted. Percentage of inhibition is referred versus the vehicle (DMSO) treated cells.

THP-1 cells

Human THP-1 cells were grown in RPMI supplemented with 10% fetal bovine serum, 2mM L-glutamine, and antibiotics and maintained in a humidified tissue culture incubator at 37°C in 5% CO_2.

For the clonogenic assay, THP-1 cells, were plated at a density of 250 cells/plate and cultured with drugs at 0.5 μM in MethoCult™ H4435 Enriched (StemCell Technologies, Vancouver, BC) according with the manufacturer instructions for 13 days. After this time, colonies were counted. Percentage of inhibition is referred versus the vehicle (DMSO) treated cells.

Retroviral Constructs and Production of Retroviruses

shRNA constructs were prepared in the MSCV-based pLMP retroviral vector . The hairpins used in the study were # 12 and #13 (scramble ShRNAs) and 1A#3 and 1A#5 (shRNAs against KDM1A):

#12 AGTACGCGAAGAATACTATCGA

#13 AGTACGTTCAGAATATCATCGAT

1A#3 AAGTGATACTGTGCTTGTCCAC

1A#5 ATCTCAGAAGATGAGTATTATT

Supernatants from transfected Phoenix packaging cells were collected at 48 and 72h post transfection and immediately used for infections.

Retroviral Transduction of NB4 and murine myeloid cells

For **NB4 cells** infection, cells were diluted in retroviral supernatants added with 8μg/ml polybrene and seeded at 10^6 cells/well in 24-well plates. Spin infection was performed for 2 consecutive days (2 infections per day) at 1800rpm for 45min. Puromycin selection (3μg/ml) started 24h after the last cycle of infection. Assays were carried out 8 days after beginning of infection.

For **murine myeloid cells** infection, cells were seeded at a density of $2x10^6$ cells/well onto RetroNectin-coated (Takara Bio Inc, Japan) non-treated 24-well plates (Corning® Costar®). Spin infection was performed as for NB4 cells. 24h after the last cycle of infection cells were seeded as for clonogenic assay in the presence of 3μg/ml of puromycin. After 7 days colonies were pooled and 20000 cells replated in absence of puromycin. Assays were carried out 7 days later.

Immunoblots and Antibodies

Whole cell extracts were obtained by lysis in SDS buffer (50 mM Tris HCl, 10% glycerol, 2% SDS). Proteins were separated by SDS-PAGE, blotted onto PVDF membrane and probed with the indicated antibodies. The antibodies used in the study were: anti-LSD1(KDM1A) (#2139 Cell Signalling), anti-KDM1B (Sigma HPA031269) and anti-HDAC1 (ab7028),

***In vivo* activity**

The *in vivo* activity was conducted on a mouse model as described by Minucci et al..[52] The

model is characterized by the development of a leukemia, resembling the human acute promyelocytic leukemia, which is associated to a blast infiltration of several organs as bone marrow, liver and particularly of the spleen.

For the *in vivo* analysis one million of leukemic cells (obtained from 129SvEv mice[52]) were injected intravenously into non-irradiated syngenic recipients. Mice were randomized in experimental groups of at least 6 mice and the treatment started once blast cells are detected in the recipients' peripheral blood (generally 10 days after injection). Compound **14d** and **14e** were dissolved in a vehicle comprising 40% PEG 400 in 5% glucose solution and orally administered either 5 days per week for 2 weeks at the doses of 27 mg/kg or 3 days per week for 2 weeks at the dose of 45 mg/kg. **22** was dissolved in a vehicle comprising 40% PEG 400 in 5% glucose solution and intraperitoneally administered 5 days per week for two weeks at the dose of 0.0125 mg/kg as reported by Oryzon.[73]

The survival of mice of the different experimental groups was analyzed and represented by a Kaplan–Meier survival plot. The pure 1S, 2R-enantiomer **15** was then dissolved in a vehicle comprising 40% PEG 400 in a 5% glucose solution and orally administered 3 days per week for 3 weeks at the doses of 11.25 mg/kg and 22.5 mg/kg. The survival of the mice of the different experimental groups was analyzed as in the case of compound **14d** and represented by a Kaplan–Meier survival plot.

All animal studies were carried out in compliance with Italian Legislative Decree N.116 dated January 27, 1992 and the European Communities Council Directive N.86/609/EEC concerning the protection of animals used for experimental or other scientific purposes and according to Institutional Policy Regarding the Care and Use of Laboratory Animals (project specific license number: 11/2012).

AUTHOR INFORMATION

Corresponding Authors

* **E-mail:** paola.vianello@ieo.eu (+39)-02.94375030, ciro.mercurio@ieo.eu

The authors declare no competing financial interest.

Acknowledgements

We wish to express our thanks to Paola Dalton for revising the manuscript.

This work was supported by Fondazione Cariplo (2010.0778), AIRC (**15208**), MIUR (Progetto Epigen), FIRB RBFR10ZJQT and RF-2010-2318330 Projects by MIUR, Sapienza Ateneo Project 2013, IIT-Sapienza Project, FP7 Projects BLUEPRINT/282510 and A-PARADDISE/602080, and Regione Lombardia, Fondo per la Promozione di Accordi Istituzionale, Bando di Invito di cui al Decreto n. 4779 del 14/05/2009, Progetto DiVA.

Table 1. Biochemical profile of compounds 1, 14a-k and 22

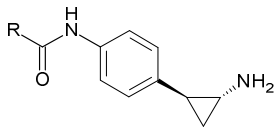

Cmpd	R	KDM1A IC50 (μM) [a]	KDM1B IC50 (μM) [a]	MAO A IC50 (μM) [a]	MAO B IC50 (μM) [a]
1		0.0192±0.004	58.3±17.4	0.0312±0.01	9.0±0.5
14a	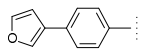	0.0225±0.001	51.0±3.1	0.0400±0.01	0.087±0.013
14b	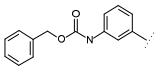	0.0426±0.01	11.6±0.2	0.0250±0.01	>100
14c	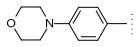	0.0615±0.006	74.7±7.00	0.0548±0.01	0.6±0.2
14d	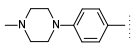	0.1885±0.104	49.3±2.8	0.7263±0.1	80.5±3.8
14e		0.0280±0.011	12.6±1.7	0.0905±0.03	80.2±15.9
14f	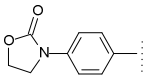	0.0335±0.002	nd	0.0297±0.01	1.6±0.5
14g		0.0512±0.024	34.7±2.8	0.5896±0.06	>100
14h	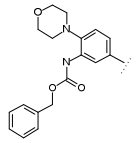	0.0614±0.011	5.7±0.6	0.1931±0.04	62.9±6.0
14i	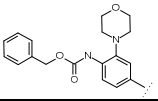	0.0750±0.011	14.9±1.8	0.3447±0.05	27.8±1.4
14j	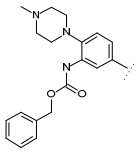	0.0890±0.02	4.3±0.8	0.9998±0.35	>100
14k	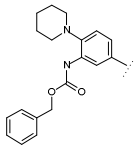	0.3075±0.069	4.3±1.0	0.6871±0.19	33.0±1.5
22		0.0065±0.001	43.45±9.6	48.38±2.19	>100

a) Data are expressed as mean of at least two determinations ± standard deviation. IC_{50} curves of biochemical assay are supplied as Supporting Information

Table 2. Cellular characterization of selected derivatives; 1, 14d-e, 14g-k

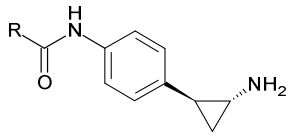

Cmpd	R	GFI1B[a]	CD11b[a]	Mouse APL blasts Methylcellulose colony formation % inhibition @ 250 nM[b]	THP-1 Methylcellulose colony formation % inhibition @ 500 nM[c]
1		4.1	2.5	73±1.0	8±6.0
14d	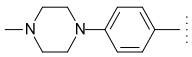	4.9	3.2	84±2.12	63±2
14e	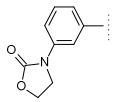	4.3	2.9	79±1.0	51±5.8
14g	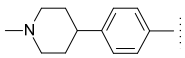	4.1	3.4	79±1.54	65±0.58
14h	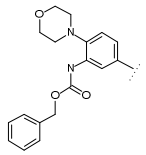	4.8	3.8	59±4.0	nd[d]
14i	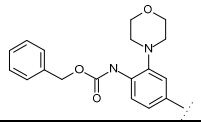	5.6	3.2	57±1.34	nd[d]
14j	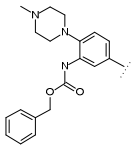	4.5	3.0	57±5.2	nd[d]
22		7.0	5.1	84±4.17	58±5.9

Percentage of inhibition is referred versus the vehicle (DMSO) treated cells and the data reported are the mean of several replicates (≥2)

a) Fold increase expressed as mean values plus standard deviation of the mRNA expression at the biochemical IC_{50}, measured after 24 h of compound treatment. The data reported are the mean of several replicates (≥2).

b) Colonies were counted after 7 days. Maximal assay variability of 4%.

c) Colonies were counted after 13 days. Maximal assay variability of 6%.

b) and c) Percentage of inhibition is referred to the vehicle (DMSO), treated cells and the data reported are the mean of several replicates (≥2)

d) Not determined.

Table 3: Pharmacokinetic parameters of 14d, 14e and 14g e after Single IV and OS administration in CD-1 mice

Parameter (Unit)	14d	14e	14g
IV 5 mg/kg			
C_{max} (μM)	0.739±0.126	3.65±0.658	0.383±0.0367
$t_{1/2}$ (h)	8.09±1.02	1.92±0.40	12.3±4.31
$AUC_{0-\infty}$ (μM·h)	2.16±0.556	4.62±1.13	2.45±0.144
CL (mL/min/kg)	94.8±21.3	49.7±12.2	80.7±4.86
V_z (L/kg)	67.5±22.1	8.45±3.75	85.7±28.3
OS 15 mg/kg			
t_{max} (h)	12.0±10.4	0.667±0.289	18.0±10.4
C_{max} (μM)	0.138±0.0517	1.14±0.16	0.0588±0.00317
$AUC_{0-\infty}$ (μM·h)	2.39±0.770	7.12±2.04	0.979±0.131
F (%)	40	55.8	15.4

Table 4. Biochemical characterization of 15 and 16

Cmpd		BIOCHEMICAL DATA			
		KDM1A IC50 (μM) [a]	KDM1B IC50 (μM) [a]	MAO A IC50 (μM) [a]	MAO B IC50 (μM) [a]
15 1S,2R	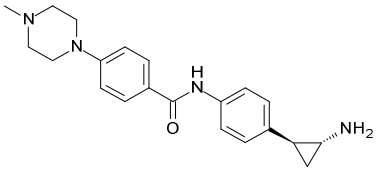	0.084±0.003	36.6±2.9	0.29±0.21	84.6±11.4
16 1R,2S	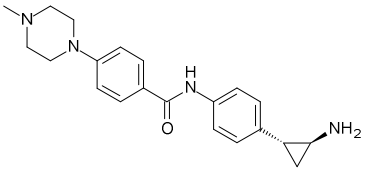	0.23±0.016	44.0±3.6	0.16±0.09	24.4±6.8

a) Data are expressed as mean of at least two determinations ± standard deviation. IC_{50} curves of biochemical assay are supplied as Supporting Information

Table 5. Cellular characterization of 15 and 16

		Target modulation		Clonogenic assay	
Cmpd		**GFI1B[a]**	**CD11b[a]**	**Mouse APL blasts Methylcellulose colony formation % inhibition @ 250 nM[b]**	**THP-1 Methylcellulose colony formation % inhibition @ 500 nM[c]**
15 1S,2R	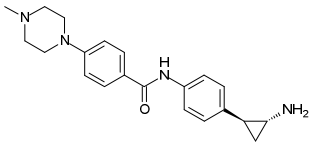	4.2	3.9	85±0.57	60±2.9
16 1R,2S	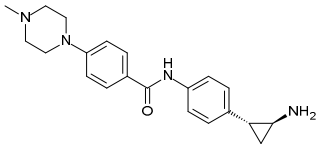	3.0	3.1	66±2.36	15±4.4

a) Fold increase expressed as mean values plus standard deviation of the mRNA expression at the biochemical IC_{50}, measured after 24 h of compound treatment. The data reported are the mean of several replicates (≥2).

b) Colonies were counted after 7 days. Percentage of inhibition is referred versus the vehicle (DMSO) treated cells and the data reported are the mean of several replicates (≥2) with a maximal assay variability of 4%.

c) Colonies were counted after 13 days. Percentage of inhibition is referred versus the vehicle (DMSO) treated cells and the data reported are the mean of several replicates (≥2) with a maximal assay variability of 6%.

Table 6: Pharmacokinetic parameters of 15 after Single IV and OS administration in CD-1 mice

Parameter (Unit)	15
IV 5 mg/kg	
C_{max} (μM)	1.92±0.883
$t_{1/2}$ (h)	8.52±1.08
$AUC_{0-\infty}$ (μM·h)	2.29±0.484
CL (mL/min/kg)	79.7± 15.0
V_z (L/kg)	58.4±9.78
OS 15 mg/kg	
C_{max} (μM)	0.147±0.112
$AUC_{0-\infty}$ (μM·h)	1.66±0.889
F (%)	22.5

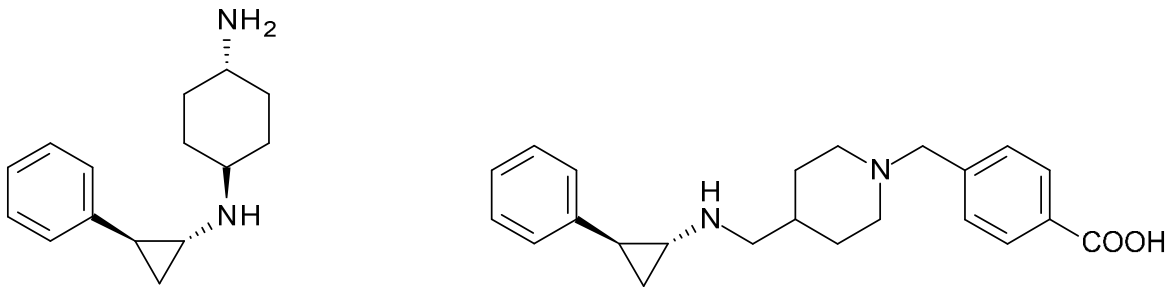

22 **23**

ORY1001/RG-6016 **GSK2879552**

Figure.1. KDM1A inhibitors in clinical studies

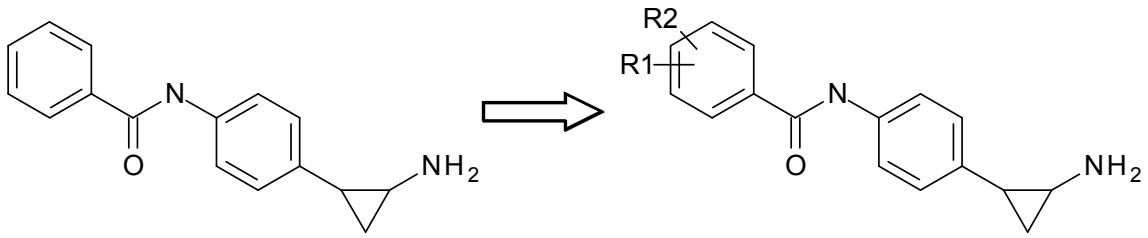

1 **14a-k**

Figure.2 Novel compounds synthesized

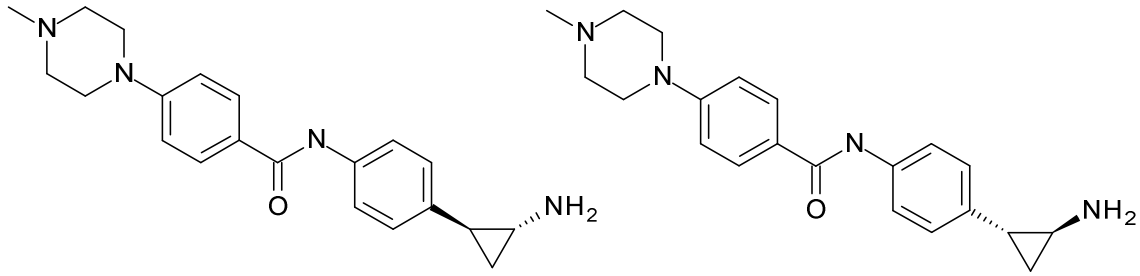

15 **16**

Figure.3 Enantiomers of compound **14d**

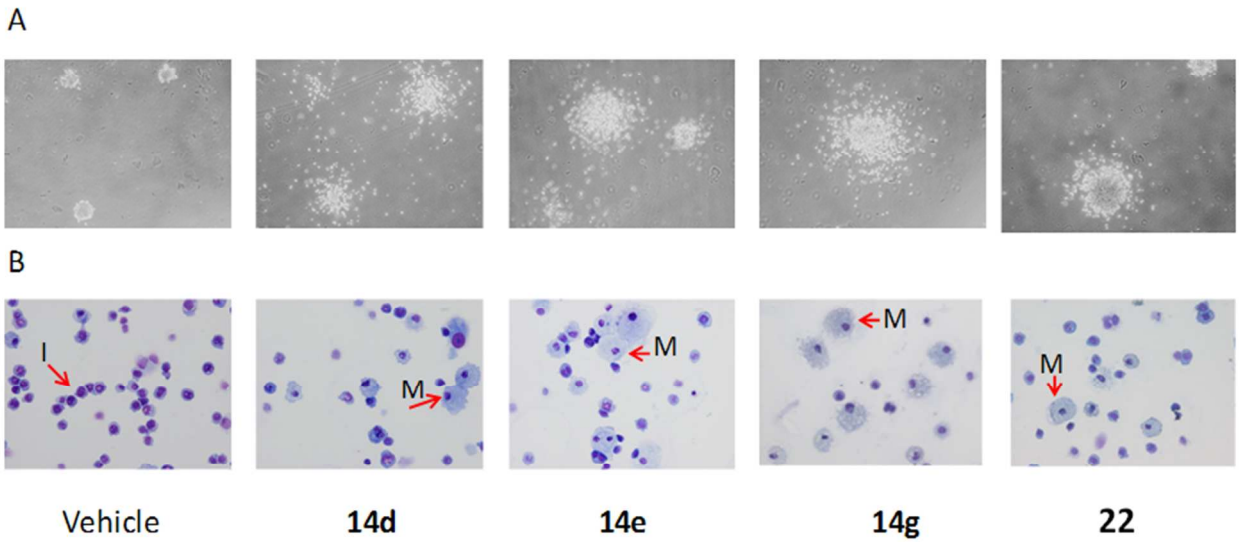

Figure 4. 14d, 14e 14g and 22 induce differentiation of THP-1 cells

A) Representative images of THP-1 colonies after 13 days in semi-solid culture with the indicated inhibitors

B) Representative images of cytospin preparations of THP-1 cells recovered at the end of semi-solid culture assay and May Grunwald-Giemsa stained. I: Immature cells; M: macrophage

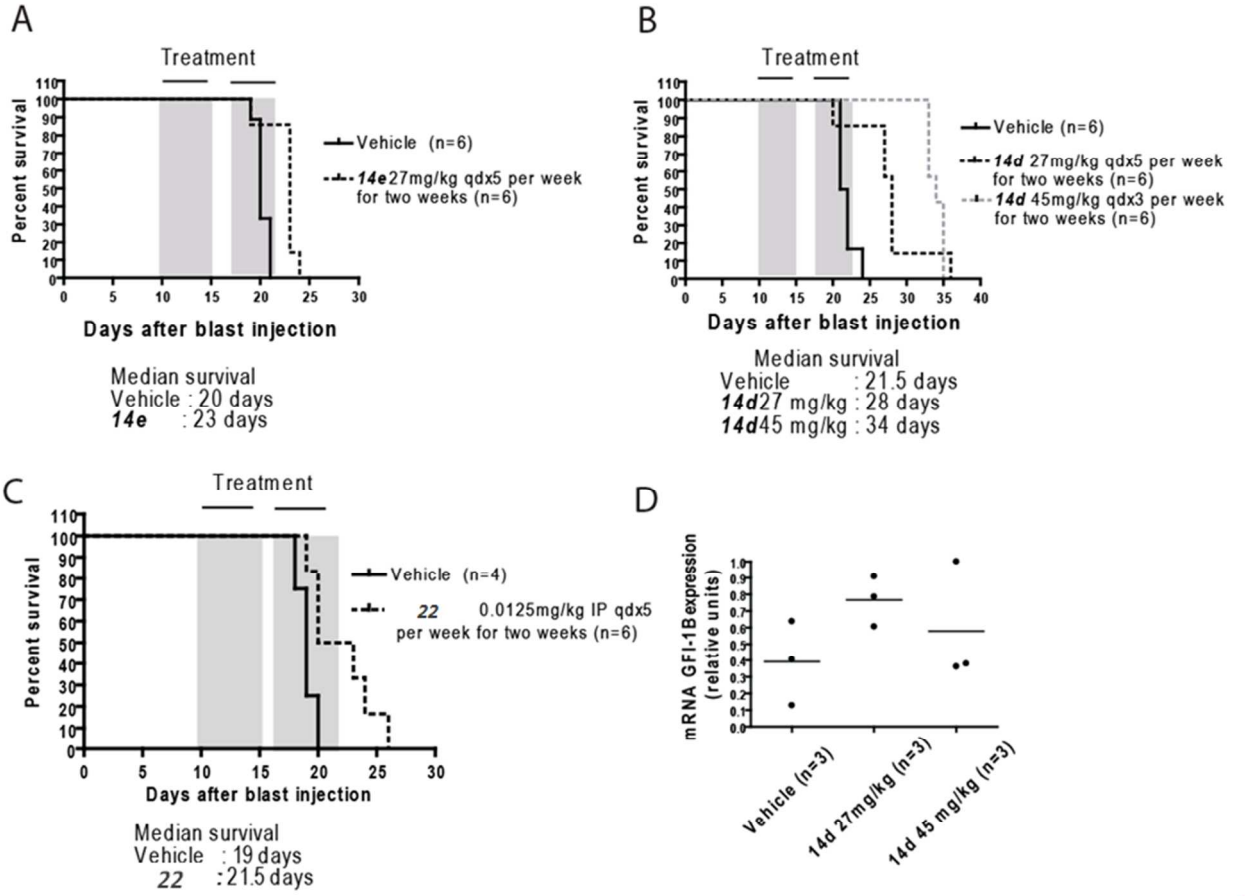

Figure 5. In vivo studies of compounds **14e**, **14d** and **22**

A) In vivo efficacy experiment in an established murine promyelocytic leukemia model of **14e**. Kaplan-Meier survival curves of leukemic mice treated with compound **14e** and its respective vehicle. Treatment started once blast cells are detected in the recipients' peripheral blood (10 days after cell injection). **14e** was orally administered at the dose of 27 mg/kg for 5 days per week for two weeks.

B) In vivo efficacy experiment in an established murine promyelocytic leukemia model of **14d**. Kaplan-Meier survival curves of leukemic mice treated with compound **14d** and its respective vehicle. Treatment started once blast cells are detected in the recipients' peripheral blood (10 days after cell injection). **14d** was orally administered at the dose of 27 mg/kg for five days per week for two weeks and at the dose of 45 mg/kg for three days per week for two weeks.

C) In vivo efficacy experiment in an established murine promyelocytic leukemia model of **22.** Kaplan-Meier survival curves of leukemic mice treated with **22** and its respective vehicle. Treatment started once blast cells are detected in the recipients' peripheral blood (10 days after cell injection). **22** was intraperitoneally administered at the dose of 0.0125 mg/kg for 5 days per week for two weeks

D) Quantitative real-time PCR analysis of GFI1B mRNA expression in leukemic cells recovered from infiltrated spleen at three days after starting in vivo treatment with compound **14d**

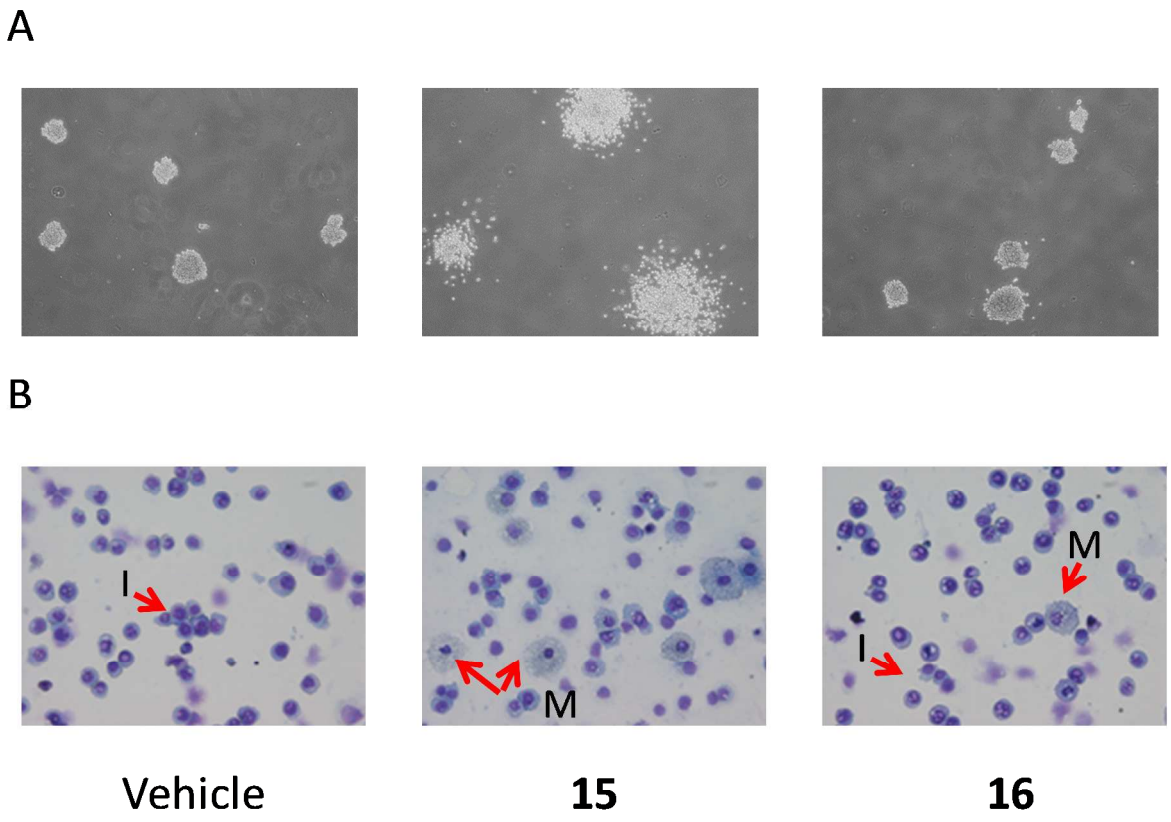

Figure 6. 15 and **16** induce differentiation of THP-1 cells.

A) Representative images of THP-1 colonies after 13 days in semi-solid culture with the indicated inhibitors

B) Representative images of cytospin preparations of THP-1 cells recovered at the end of semi-solid culture assay and May Grunwald-Giemsa stained. I: Immature cells; M: macrophage

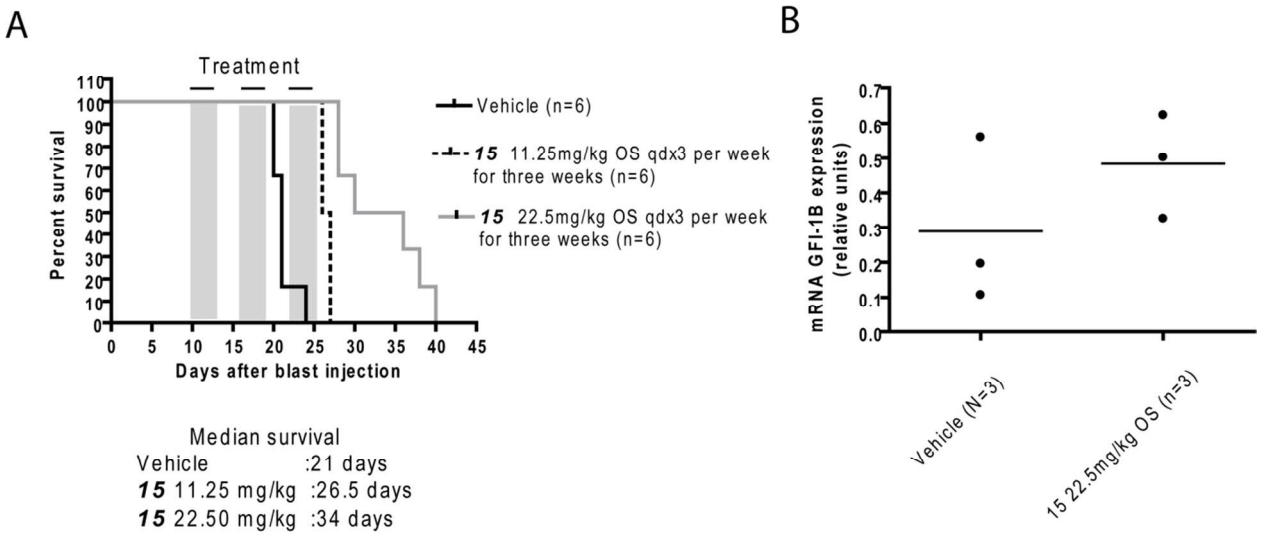

Figure7. In vivo studies of compound **15**

A) In vivo efficacy experiment in an established murine promyelocytic leukemia model of **15**. Kaplan-Meier survival curves of leukemic mice treated with compound **15** and its respective vehicle. Treatment started once blast cells are detected in the recipients' peripheral blood (10 days after cell injection). **15** was orally administered at the doses of 11.25 and 22.5 mg/kg for three days per week for three weeks.

B) Quantitative real-time PCR analysis of GFI1B mRNA expression in leukemic cells recovered from infiltrated spleen at three days after starting in vivo treatment with compound **15.**

Scheme 1

Method A

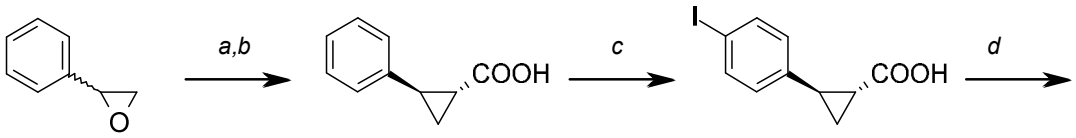

2 (racemic)
3 (2S)
4 (2R)

5 (trans racemic)
6 (1R, 2R)
7 (1S, 2S)

8 (trans racemic)
9 (1R, 2R)
10 (1S, 2S)

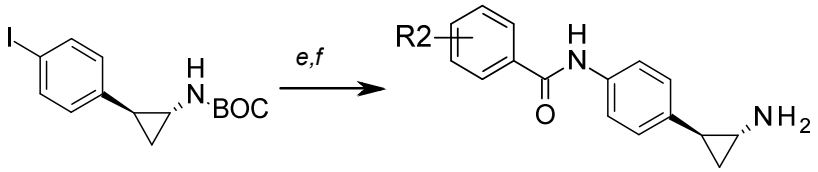

11 (trans racemic)
12 (1R, 2S)
13 (1S, 2R)

14a-g (trans racemic)
15 (1S, 2R)
16 (1R, 2S)

Reagents and conditions: a) Triethyl phosphonoacetate, BuLi, DME, 135°C, mw, 1 h; b) LiOH, THF, water, EtOH, mw, 115°C, 50 min; c) I_2, KIO_3, H_2O, CH_3COOH, H_2SO_4, 2 h, 0°C, reflux; d) DPPA, tBuOH, TEA, 90°C, 20 h; e) $ArCONH_2$, CuI, DMEDA, K_2CO_3, Dioxane, 110°C, 20 h; f) HCl, MeOH, diethylether, 0°C, 20 h

Scheme 2

Method B

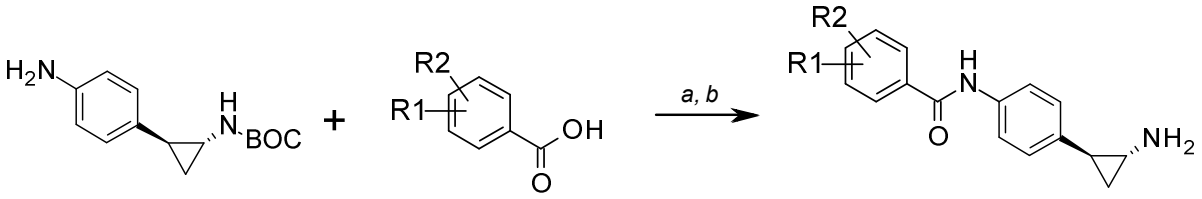

17 **18h-k** **14h-k**

Reagents and conditions: a) PyBOP, TEA, DMF, RT, overnight; b) THF, 4 M HCl in dioxane, RT, overnight.

Scheme 3

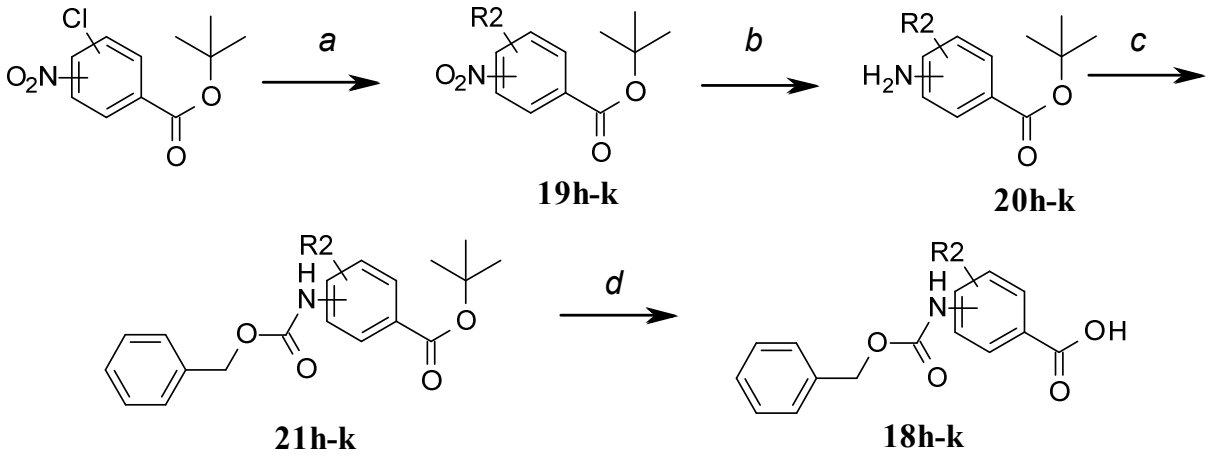

Reagents and conditions: a) morpholine, 4-methylpiperazine, or piperidine, K_2CO_3, DMF,90 °C. 5 h, b) 10%Pd-C, MeOH, Parr apparatus, 50 psi, 25°C, 5h; c) Benzyl chloroformate, TEA, THF, RT 1.5 h; d) TFA, CH_2Cl_2, RT, overnight.

Scheme 4

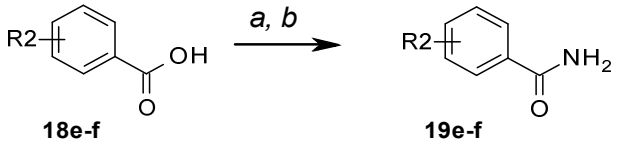

Reagents and conditions: a) thionyl chloride, DMF, CH_2Cl_2, reflux, 2h. b) NH_3 (28-30% in water), RT 1h

ASSOCIATED CONTENT

Supporting Information

Additional figures illustrating: 1) IC50 curves of biochemical assay, 2) effect of KDM1A down regulation on mRNA expression of GFI1B and CD11b in NB4 cells and 3) effect of KDM1A

down regulation on clonogenic potential of mouse promyelocytic blasts. This material is available free of charge via the Internet at http://pubs.acs.org.

AUTHOR INFORMATION

Corresponding Authors

*** E-mail:** paola.vianello@ieo.eu (+39)-02.94375030, ciro.mercurio@ieo.eu

The authors declare no competing financial interest.

Funding Sources

This work was supported by Fondazione Cariplo (2010.0778), AIRC (**15208**), MIUR (Progetto Epigen), FIRB RBFR10ZJQT and RF-2010-2318330 Projects by MIUR, Sapienza Ateneo Project 2013, IIT-Sapienza Project, FP7 Projects BLUEPRINT/282510 and A-PARADDISE/602080, and Regione Lombardia, Fondo per la Promozione di Accordi Istituzionale, Bando di Invito di cui al Decreto n. 4779 del 14/05/2009, Progetto DiVA.

Acknowledgements

We wish to express our thanks to Paola Dalton for revising the manuscript.

ABBREVIATIONS USED

AML, Acute Myeloid Leukemia; APL, Acute Promyelocytic Leukemia; br s, broad signal; n-BuLi, n-butyllithium; CH_2Cl_2, dichloromethane; DPPA, diphenylphosphoryl azide; DMEDA, 2-(Dimethylamino)ethylamine; MeOH, Methanol; mp, melting point; PyBOP, (Benzotriazol-1-yloxy)tripyrrolidinophosphonium hexafluorophosphate; RT, room temperature; tBuOH, tert-Butanol; TCPA, tranylcypromine; TEA, triethylamine; THF, tetrahydrofuran.

REFERENCES

1. Helin, K.; Dhanak, D. Chromatin proteins and modifications as drug targets. Nature 2013, *502*, 480-488.

2. Jones, P. A.; Baylin, S. B. The epigenomics of cancer. Cell 2007, *128*, 683-692.

3. Rodriguez-Paredes, M.; Esteller, M. Cancer epigenetics reaches mainstream oncology. Nat Med 2011, *17*, 330-339.

4. Black, J. C.; Van Rechem, C.; Whetstine, J. R. Histone lysine methylation dynamics: establishment, regulation, and biological impact. Mol Cell 2012, *48*, 491-507.

5. Greer, E. L.; Shi, Y. Histone methylation: a dynamic mark in health, disease and inheritance. Nat Rev Genet 2012, *13*, 343-357.

6. Huang, H.; Sabari, B. R.; Garcia, B. A.; Allis, C. D.; Zhao, Y. SnapShot: histone modifications. Cell 2014, *159*, 458-458 e1.

7. Cheng, X.; Collins, R. E.; Zhang, X. Structural and sequence motifs of protein (histone) methylation enzymes. Annu Rev Biophys Biomol Struct 2005, *34*, 267-294.

8. Klose, R. J.; Kallin, E. M.; Zhang, Y. JmjC-domain-containing proteins and histone demethylation. Nat Rev Genet 2006, *7*, 715-727.

9. Kooistra, S. M.; Helin, K. Molecular mechanisms and potential functions of histone demethylases. Nat Rev Mol Cell Biol 2012, *13*, 297-311.

10. Shi, Y.; Lan, F.; Matson, C.; Mulligan, P.; Whetstine, J. R.; Cole, P. A.; Casero, R. A. Histone demethylation mediated by the nuclear amine oxidase homolog LSD1. Cell 2004, *119*, 941-953.

11. Karytinos, A.; Forneris, F.; Profumo, A.; Ciossani, G.; Battaglioli, E.; Binda, C.; Mattevi, A. A novel mammalian flavin-dependent histone demethylase. J Biol Chem 2009, *284*, 17775-17782.

12. Lee, M. G.; Wynder, C.; Cooch, N.; Shiekhattar, R. An essential role for CoREST in nucleosomal histone 3 lysine 4 demethylation. Nature 2005, *437,* 432-435.

13. Shi, Y. J.; Matson, C.; Lan, F.; Iwase, S.; Baba, T.; Shi, Y. Regulation of LSD1 histone demethylase activity by its associated factors. Mol Cell 2005, *19*, 857-864.

14. You, A.; Tong, J. K.; Grozinger, C. M.; Schreiber, S. L. CoREST is an integral component of the CoREST- human histone deacetylase complex. Proc Natl Acad Sci U S A 2001, *98*, 1454-1458.

15. Wang, Y.; Zhang, H.; Chen, Y.; Sun, Y.; Yang, F.; Yu, W.; Liang, J.; Sun, L.; Yang, X.; Shi, L.; Li, R.; Li, Y.; Zhang, Y.; Li, Q.; Yi, X.; Shang, Y. LSD1 is a subunit of the NuRD complex and targets the metastasis programs in breast cancer. Cell 2009, *138*, 660-672.

16. Tong, J. K.; Hassig, C. A.; Schnitzler, G. R.; Kingston, R. E.; Schreiber, S. L. Chromatin deacetylation by an ATP-dependent nucleosome remodelling complex. Nature 1998, *395*, 917-921.

17. Barski, A.; Cuddapah, S.; Cui, K.; Roh, T. Y.; Schones, D. E.; Wang, Z.; Wei, G.; Chepelev, I.; Zhao, K. High-resolution profiling of histone methylations in the human genome. Cell 2007, *129*, 823-837.

18. Metzger, E.; Wissmann, M.; Yin, N.; Muller, J. M.; Schneider, R.; Peters, A. H.; Gunther, T.; Buettner, R.; Schule, R. LSD1 demethylates repressive histone marks to promote androgen-receptor-dependent transcription. Nature 2005, *437*, 436-439.

19. Nair, S. S.; Nair, B. C.; Cortez, V.; Chakravarty, D.; Metzger, E.; Schule, R.; Brann, D. W.; Tekmal, R. R.; Vadlamudi, R. K. PELP1 is a reader of histone H3 methylation that facilitates oestrogen receptor-alpha target gene activation by regulating lysine demethylase 1 specificity. EMBO Rep 2010, *11*, 438-444.

20. Biswas, D.; Milne, T. A.; Basrur, V.; Kim, J.; Elenitoba-Johnson, K. S.; Allis, C. D.; Roeder, R. G. Function of leukemogenic mixed lineage leukemia 1 (MLL) fusion proteins through distinct partner protein complexes. Proc Natl Acad Sci U S A 2011, *108*, 15751-15756.

21. Nakamura, T.; Mori, T.; Tada, S.; Krajewski, W.; Rozovskaia, T.; Wassell, R.; Dubois, G.; Mazo, A.; Croce, C. M.; Canaani, E. ALL-1 is a histone methyltransferase that assembles a supercomplex of proteins involved in transcriptional regulation. Mol Cell 2002, *10*, 1119-1128.

22. Lee, M. G.; Wynder, C.; Schmidt, D. M.; McCafferty, D. G.; Shiekhattar, R. Histone H3 lysine 4 demethylation is a target of nonselective antidepressive medications. Chem Biol 2006, *13*, 563-567.

23. Forneris, F.; Binda, C.; Vanoni, M. A.; Battaglioli, E.; Mattevi, A. Human histone demethylase LSD1 reads the histone code. J Biol Chem 2005, *280*, 41360-41365.

24. Cho, H. S.; Suzuki, T.; Dohmae, N.; Hayami, S.; Unoki, M.; Yoshimatsu, M.; Toyokawa, G.; Takawa, M.; Chen, T.; Kurash, J. K.; Field, H. I.; Ponder, B. A.; Nakamura, Y.; Hamamoto, R. Demethylation of RB regulator MYPT1 by histone demethylase LSD1 promotes cell cycle progression in cancer cells. Cancer Res 2011, *71*, 655-660.

25. Huang, J.; Sengupta, R.; Espejo, A. B.; Lee, M. G.; Dorsey, J. A.; Richter, M.; Opravil, S.; Shiekhattar, R.; Bedford, M. T.; Jenuwein, T.; Berger, S. L. p53 is regulated by the lysine demethylase LSD1. Nature 2007, *449*, 105-108.

26. Kontaki, H.; Talianidis, I. Lysine methylation regulates E2F1-induced cell death. Mol Cell 2010, *39*, 152-160.

27. Wang, J.; Hevi, S.; Kurash, J. K.; Lei, H.; Gay, F.; Bajko, J.; Su, H.; Sun, W.; Chang, H.; Xu, G.; Gaudet, F.; Li, E.; Chen, T. The lysine demethylase LSD1 (KDM1) is required for maintenance of global DNA methylation. Nat Genet 2009, *41*, 125-129.

28. Yang, J.; Huang, J.; Dasgupta, M.; Sears, N.; Miyagi, M.; Wang, B.; Chance, M. R.; Chen, X.; Du, Y.; Wang, Y.; An, L.; Wang, Q.; Lu, T.; Zhang, X.; Wang, Z.; Stark, G. R. Reversible methylation of promoter-bound STAT3 by histone-modifying enzymes. Proc Natl Acad Sci U S A 2010, *107*, 21499-21504.

29. Schulte, J. H.; Lim, S.; Schramm, A.; Friedrichs, N.; Koster, J.; Versteeg, R.; Ora, I.; Pajtler, K.; Klein-Hitpass, L.; Kuhfittig-Kulle, S.; Metzger, E.; Schule, R.; Eggert, A.; Buettner, R.; Kirfel, J. Lysine-specific demethylase 1 is strongly expressed in poorly differentiated neuroblastoma: implications for therapy. Cancer Res 2009, *69*, 2065-2071.

30. Kahl, P.; Gullotti, L.; Heukamp, L. C.; Wolf, S.; Friedrichs, N.; Vorreuther, R.; Solleder, G.; Bastian, P. J.; Ellinger, J.; Metzger, E.; Schule, R.; Buettner, R. Androgen receptor coactivators lysine-specific histone demethylase 1 and four and a half LIM domain protein 2 predict risk of prostate cancer recurrence. Cancer Res 2006, *66*, 11341-11347.

31. Lv, T.; Yuan, D.; Miao, X.; Lv, Y.; Zhan, P.; Shen, X.; Song, Y. Over-expression of LSD1 promotes proliferation, migration and invasion in non-small cell lung cancer. PLoS One 2012, *7*, e35065.

32. Derr, R. S.; van Hoesel, A. Q.; Benard, A.; Goossens-Beumer, I. J.; Sajet, A.; Dekker-Ensink, N. G.; de Kruijf, E. M.; Bastiaannet, E.; Smit, V. T.; van de Velde, C. J.; Kuppen, P. J. High nuclear expression levels of histone-modifying enzymes LSD1, HDAC2 and SIRT1 in tumor cells correlate with decreased survival and increased relapse in breast cancer patients. BMC Cancer 2014, *14*, 604.

33. Lim, S.; Janzer, A.; Becker, A.; Zimmer, A.; Schule, R.; Buettner, R.; Kirfel, J. Lysine-specific demethylase 1 (LSD1) is highly expressed in ER-negative breast cancers and a biomarker predicting aggressive biology. Carcinogenesis 2010, *31*, 512-520.

34. Yu, Y.; Wang, B.; Zhang, K.; Lei, Z.; Guo, Y.; Xiao, H.; Wang, J.; Fan, L.; Lan, C.; Wei, Y.; Ma, Q.; Lin, L.; Mao, C.; Yang, X.; Chen, X.; Li, Y.; Bai, Y.; Chen, D. High expression of lysine-specific demethylase 1 correlates with poor prognosis of patients with esophageal squamous cell carcinoma. Biochem Biophys Res Commun 2013, *437*, 192-198.

35. Zhao, Z. K.; Yu, H. F.; Wang, D. R.; Dong, P.; Chen, L.; Wu, W. G.; Ding, W. J.; Liu, Y. B. Overexpression of lysine specific demethylase 1 predicts worse prognosis in primary hepatocellular carcinoma patients. World J Gastroenterol 2012, *18*, 6651-6656.

36. Hayami, S.; Kelly, J. D.; Cho, H. S.; Yoshimatsu, M.; Unoki, M.; Tsunoda, T.; Field, H. I.; Neal, D. E.; Yamaue, H.; Ponder, B. A.; Nakamura, Y.; Hamamoto, R. Overexpression of LSD1 contributes to human carcinogenesis through chromatin regulation in various cancers. Int J Cancer 2011, *128*, 574-586.

37. Huang, Z.; Li, S.; Song, W.; Li, X.; Li, Q.; Zhang, Z.; Han, Y.; Zhang, X.; Miao, S.; Du, R.; Wang, L. Lysine-specific demethylase 1 (LSD1/KDM1A) contributes to colorectal tumorigenesis via activation of the Wnt/beta-catenin pathway by down-regulating Dickkopf-1 (DKK1) [corrected]. PLoS One 2013, *8*, e70077.

38. Wu, Y.; Wang, Y.; Yang, X. H.; Kang, T.; Zhao, Y.; Wang, C.; Evers, B. M.; Zhou, B. P. The deubiquitinase USP28 stabilizes LSD1 and confers stem-cell-like traits to breast cancer cells. Cell Rep 2013, *5*, 224-236.

39. Suva, M. L.; Rheinbay, E.; Gillespie, S. M.; Patel, A. P.; Wakimoto, H.; Rabkin, S. D.; Riggi, N.; Chi, A. S.; Cahill, D. P.; Nahed, B. V.; Curry, W. T.; Martuza, R. L.; Rivera, M. N.; Rossetti, N.; Kasif, S.; Beik, S.; Kadri, S.; Tirosh, I.; Wortman, I.; Shalek, A. K.; Rozenblatt-Rosen, O.; Regev, A.; Louis, D. N.; Bernstein, B. E. Reconstructing and reprogramming the tumor-propagating potential of glioblastoma stem-like cells. Cell 2014, *157*, 580-594.

40. Lynch, J. T.; Harris, W. J.; Somervaille, T. C. LSD1 inhibition: a therapeutic strategy in cancer? Expert Opin Ther Targets 2012, *16*, 1239-1249.

41. Niebel, D.; Kirfel, J.; Janzen, V.; Holler, T.; Majores, M.; Gutgemann, I. Lysine-specific demethylase 1 (LSD1) in hematopoietic and lymphoid neoplasms. Blood 2014, *124*, 151-152.

42. Harris, W. J.; Huang, X.; Lynch, J. T.; Spencer, G. J.; Hitchin, J. R.; Li, Y.; Ciceri, F.; Blaser, J. G.; Greystoke, B. F.; Jordan, A. M.; Miller, C. J.; Ogilvie, D. J.; Somervaille, T. C. The histone demethylase KDM1A sustains the oncogenic potential of MLL-AF9 leukemia stem cells. Cancer Cell 2012, *21*, 473-487.

43. Benelkebir, H.; Hodgkinson, C.; Duriez, P. J.; Hayden, A. L.; Bulleid, R. A.; Crabb, S. J.; Packham, G.; Ganesan, A. Enantioselective synthesis of tranylcypromine analogues as lysine demethylase (LSD1) inhibitors. Bioorg Med Chem 2011, *19*, 3709-3716.

44. Gooden, D. M.; Schmidt, D. M.; Pollock, J. A.; Kabadi, A. M.; McCafferty, D. G. Facile synthesis of substituted trans-2-arylcyclopropylamine inhibitors of the human histone demethylase LSD1 and monoamine oxidases A and B. Bioorg Med Chem Lett 2008, *18*, 3047-3051.

45. Hojfeldt, J. W.; Agger, K.; Helin, K. Histone lysine demethylases as targets for anticancer therapy. Nat Rev Drug Discov 2013, *12*, 917-930.

46. Khan, M. N.; Suzuki, T.; Miyata, N. An overview of phenylcyclopropylamine derivatives: biochemical and biological significance and recent developments. Med Res Rev 2013, *33*, 873-910.

47. Mimasu, S.; Umezawa, N.; Sato, S.; Higuchi, T.; Umehara, T.; Yokoyama, S. Structurally designed trans-2-phenylcyclopropylamine derivatives potently inhibit histone demethylase LSD1/KDM1. Biochemistry 2010, *49*, 6494-6503.

48. Mould, D. P.; McGonagle, A. E.; Wiseman, D. H.; Williams, E. L.; Jordan, A. M. Reversible Inhibitors of LSD1 as Therapeutic Agents in Acute Myeloid Leukemia: Clinical Significance and Progress to Date. Med Res Rev 2014.

49. Ogasawara, D.; Itoh, Y.; Tsumoto, H.; Kakizawa, T.; Mino, K.; Fukuhara, K.; Nakagawa, H.; Hasegawa, M.; Sasaki, R.; Mizukami, T.; Miyata, N.; Suzuki, T. Lysine-specific demethylase 1-selective inactivators: protein-targeted drug delivery mechanism. Angew Chem Int Ed Engl 2013, *52*, 8620-8624.

50. Pieroni, M.; Annunziato, G.; Azzali, E.; Dessanti, P.; Mercurio, C.; Meroni, G.; Trifiro, P.; Vianello, P.; Villa, M.; Beato, C.; Varasi, M.; Costantino, G. Further insights into the SAR of alpha-substituted cyclopropylamine derivatives as inhibitors of histone demethylase KDM1A. Eur J Med Chem 2015, *92*, 377-386.

51. Johnson, N. W.; Kasparec, J.; Miller, W. H.; Rouse, M.; Suarez, D.; Tian, X. Cyclopropylamines as LSD1 Inhibitors. WO2012/135113, 04-10-2012, 2012.

52. Maes, T.; Martinell Pedemonte, M. Lysine Demethylase Inhibitors for Thrombosis and Cardiovascular Diseases. WO2012/156537, 22-11-2012, 2012.

53. Maes, T.; Martinell Pedemonte, M. Lysine Demethylase Inhibitors for Inflammatory Diseases or Conditions. WO2012/156531, 22-11-2012, 2012.

54. Ortega Munoz, A.; Fyfe, M. C. T.; Estiarte Martinez, M. d. L. A.; Valls Vidal, N.; Kurz, G.; Castro Palomino, L. J. C. (Hetero)Aryl Cyclopropylamine Compounds as LSD1 Inhibitors. WO2013/057320, 25-04-2013, 2013.

55. Ortega Munoz, A.; Fyfe, M. C. T.; martinell Pedemonte, M.; Estiarte Martinez, M. d. L. A.; Valls Vidal, N.; Kurz, G.; Castro Palomino, L. J. C. (Hetero)Aryl Cyclopropylamine Compounds as LSD1 Inhibitors. WO2013/057322, 25-04-2013, 2013.

56. Tomita, N.; Shigeo, K. Cyclopropaneamine Compound. WO2013/022047, 14-02-2013, 2013.

57. https://www.clinicaltrialsregister.eu/ctr-search/trial/2013-002447-29/ES

A phase I study of Human Pharmacokinetics and Safety of ORY-1001, an LSD1 inhibitor, in relapsed or refractory acute leukaemia (AL). EudraCT number 2013-002447-29.

58. Maes, T.; Carceller, E.; Salas, J.; Ortega, A.; Buesa, C. Advances in the development of histone lysine demethylase inhibitors. Curr Opin Pharmacol 2015, *23*, 52-60.

59. McGrath, J.; Trojer, P. Targeting histone lysine methylation in cancer. Pharmacol Ther 2015, *150*, 1-22.

60.https://clinicaltrials.gov/ct2/show/NCT02034123?term=GSK2879552&rank=1Investigation of GSK2879552 in Subjects With Relapsed/Refractory Small Cell Lung Carcinoma.

61. https://clinicaltrials.gov/ct2/show/NCT02177812?term=GSK2879552&rank=2

Phase I Dose Escalation Study for GSK2879552 in Subjects With Acute Myeloid Leukemia (AML) ClinicalTrials.gov Identifier: NCT02177812.

62. Mohammad, H. P.; Smitheman, K. N.; Kamat, C. D.; Soong, D.; Federowicz, K. E.; Van Aller, G. S.; Schneck, J. L.; Carson, J. D.; Liu, Y.; Butticello, M.; Bonnette, W. G.; Gorman, S. A.; Degenhardt, Y.; Bai, Y.; McCabe, M. T.; Pappalardi, M. B.; Kasparec, J.; Tian, X.; McNulty,

K. C.; Rouse, M.; McDevitt, P.; Ho, T.; Crouthamel, M.; Hart, T. K.; Concha, N. O.; McHugh, C. F.; Miller, W. H.; Dhanak, D.; Tummino, P. J.; Carpenter, C. L.; Johnson, N. W.; Hann, C. L.; Kruger, R. G. A DNA Hypomethylation Signature Predicts Antitumor Activity of LSD1 Inhibitors in SCLC. Cancer Cell 2015, *28*, 57-69.

63. Mould, D. P.; McGonagle, A. E.; Wiseman, D. H.; Williams, E. L.; Jordan, A. M. Reversible inhibitors of LSD1 as therapeutic agents in acute myeloid leukemia: clinical significance and progress to date. Med Res Rev 2015, *35*, 586-618.

64. Binda, C.; Valente, S.; Romanenghi, M.; Pilotto, S.; Cirilli, R.; Karytinos, A.; Ciossani, G.; Botrugno, O. A.; Forneris, F.; Tardugno, M.; Edmondson, D. E.; Minucci, S.; Mattevi, A.; Mai, A. Biochemical, structural, and biological evaluation of tranylcypromine derivatives as inhibitors of histone demethylases LSD1 and LSD2. J Am Chem Soc 2010, *132*, 6827-6833.

65. Valente, S.; Rodriguez, V.; Mercurio, C.; Vianello, P.; Saponara, B.; Cirilli, R.; Ciossani, G.; Labella, D.; Marrocco, B.; Monaldi, D.; Ruoppolo, G.; Tilset, M.; Botrugno, O. A.; Dessanti, P.; Minucci, S.; Mattevi, A.; Varasi, M.; Mai, A. Pure enantiomers of benzoylamino-tranylcypromine: LSD1 inhibition, gene modulation in human leukemia cells and effects on clonogenic potential of murine promyelocytic blasts. Eur J Med Chem 2015, *94*, 163-174.

66. Bujok, R. Novel approach to synthesis of substituted 3-aminoquinolines from nitroarenes and protected ethyl aminocrotonate. Tetrahedron 2010, *66*, 698–708.

67. Taylor, R. D.; MacCoss, M.; Lawson, A. D. Rings in drugs. J Med Chem 2014, *57*, 5845-5859.

68. Binda, C.; Newton-Vinson, P.; Hubalek, F.; Edmondson, D. E.; Mattevi, A. Structure of human monoamine oxidase B, a drug target for the treatment of neurological disorders. Nat Struct Biol 2002, *9*, 22-26.

69. Vianello, P.; Botrugno, O. A.; Cappa, A.; Ciossani, G.; Dessanti, P.; Mai, A.; Mattevi, A.; Meroni, G.; Minucci, S.; Thaler, F.; Tortorici, M.; Trifiro, P.; Valente, S.; Villa, M.; Varasi, M.; Mercurio, C. Synthesis, biological activity and mechanistic insights of 1-substituted cyclopropylamine derivatives: a novel class of irreversible inhibitors of histone demethylase KDM1A. Eur J Med Chem 2014, *86*, 352-363.

70. Saleque, S.; Kim, J.; Rooke, H. M.; Orkin, S. H. Epigenetic regulation of hematopoietic differentiation by Gfi-1 and Gfi-1b is mediated by the cofactors CoREST and LSD1. Mol Cell 2007, *27*, 562-572.

71. Minucci, S.; Monestiroli, S.; Giavara, S.; Ronzoni, S.; Marchesi, F.; Insinga, A.; Diverio, D.; Gasparini, P.; Capillo, M.; Colombo, E.; Matteucci, C.; Contegno, F.; Lo-Coco, F.; Scanziani, E.; Gobbi, A.; Pelicci, P. G. PML-RAR induces promyelocytic leukemias with high efficiency following retroviral gene transfer into purified murine hematopoietic progenitors. Blood 2002, *100*, 2989-2995.

72. Leiva, M.; Moretti, S.; Soilihi, H.; Pallavicini, I.; Peres, L.; Mercurio, C.; Dal Zuffo, R.; Minucci, S.; de The, H. Valproic acid induces differentiation and transient tumor regression, but spares leukemia-initiating activity in mouse models of APL. Leukemia 2012, *26*, 1630-1637.

73. Maes, T.; Tirapu, I.; Mascarò, C.; Ortega, A.; Estiarte, A.; Valls, N.; Castro Palomino, J.; Arjol, C. B.; Kurz, G. Preclinical characterization of a potent and selective inhibitor of the histone demethylase KDM1A for MLL leukemia. J Clin Oncol 2013, 31, suppl; abstr e13543.

74. Brucoli, F.; Howard, P. W.; Thurston, D. E. Efficient solid-phase synthesis of a library of distamycin analogs containing novel biaryl motifs on SynPhase Lanterns. J Comb Chem 2009, *11*, 576-586.

75. Shearer, B. G.; Chao, E. Y.; Uehling, D. E.; Deaton, D. N.; Cowan, C.; Sherman, B. W.; Milliken, T.; Faison, W.; Brown, K.; Adkison, K. K.; Lee, F. Synthesis and evaluation of potent and selective beta3 adrenergic receptor agonists containing heterobiaryl carboxylic acids. Bioorg Med Chem Lett 2007, *17*, 4670-4677.

Table of Contents Graphic

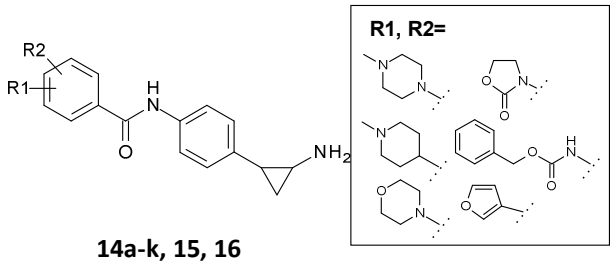

14a-k, 15, 16

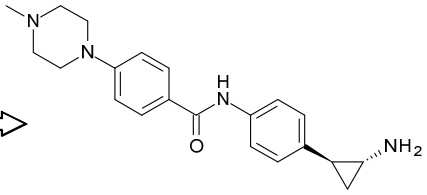

15

***Biochemical assay*: KDM1A** IC50=0.084μM
***Cellular assay*: APL blast** 85% inhibition (at 250nM)
THP1 60% inhibition (at 500nM)
In Vivo: **Prolonged Survival Time** 62% (at 22.50 mg/kg)